The Journal of Neuroscience, April 1994, 14(4): 2383–2401

$GABA_A$ Receptor Subunit Immunoreactivity in Primate Visual Cortex: Distribution in Macaques and Humans and Regulation by Visual Input in Adulthood

S. H. C. Hendry,[1] M.-M. Huntsman,[1] A. Viñuela,[1] H. Möhler,[2] A. L. de Blas,[3] and E. G. Jones[1]

[1]Department of Anatomy and Neurobiology, University of California at Irvine, Irvine, California 92717, [2]Institute of Pharmacology, University of Zürich, CH-8057 Zürich, Switzerland, and [3]Division of Molecular Biology, University of Missouri at Kansas City, Kansas City, Missouri 64110

Subunit proteins that make up functional $GABA_A$ receptors were localized by immunocytochemistry in the primary visual cortex (area 17) of adult monkeys and humans. Immunoreactivity for the $\alpha 1$, $\beta 2/3$, and $\gamma 2$ subunits is greatest in layers (II–III, IVA and IVC) of monkey area 17 that contain the highest density of GABA neurons and terminals. Immunostaining for each subunit is unevenly distributed in layers II and III, where patches of immunoreactivity correspond to regions of intense cytochrome oxidase (CO) staining, and in layer IVA, where intense immunoreactivity forms a honeycomb pattern identical to the CO staining pattern. Immunoreactivity for the subunits is localized principally within the neuropil, which, by simultaneous comparison with the distribution of microtubule-associated protein immunostaining, was found to include bundles of thin dendrites and zones of numerous dendritic segments. In addition, $\gamma 2$ immunostaining surrounds the somata of a subpopulation of GABAergic neurons, immunoreactive for the calcium-binding protein parvalbumin. All three subunits are present in the somata and processes of neurons that occupy the white matter subjacent to monkey area 17.

In human visual cortex, the $\alpha 1$, $\beta 2/3$, and $\gamma 2$ subunits are distributed in a manner similar to that found in monkeys, with relatively intense immunostaining in layers IVC and IVA. In layer IVC, vertical stripes of intense receptor immunostaining (20–30 μm wide) alternate with wider stripes of pale immunostaining (30–60 μm wide). In the upper and lower halves of IVCβ, these stripes form lattices similar to those in layers IVC and IVA of monkeys.

Following monocular deprivation by intravitreal injections of TTX in adult monkeys, immunoreactivity for each subunit in layer IVC consists of alternating intensely and lightly stained stripes. Comparison with the pattern of CO staining indicates that intense immunostaining for $\alpha 1$, $\beta 2/3$, and $\gamma 2$ occurs in normal-eye stripes while abnormally light immunostaining is present in deprived-eye stripes. For all three subunits, immunoreactivity in deprived-eye stripes is reduced within 5 d of monocular deprivation and remains abnormally low for deprivations that extend to at least 30 d.

These findings indicate that each of several $GABA_A$ receptor subunits adopt similar laminar and compartmental distributions in monkey and human area 17 and are likely to be expressed by the same neurons. The deprivation-dependent reduction in immunoreactivity for $\alpha 1$, $\beta 2/3$, and $\gamma 2$ subunits suggests that all are regulated by visually driven activity. Together with the previously observed reduction in GABA immunoreactivity, the downregulation of $GABA_A$ receptors would be expected to leave the deprived-eye column with reduced levels of GABA-mediated inhibition, most likely contributing to the functional adaptation seen in visually deprived adult monkeys.

[Key words: striate cortex, visual deprivation, neuronal plasticity, intracortical inhibition, human cerebral cortex, neurotransmitter receptor regulation]

The amino acid neurotransmitter GABA inhibits neurons of the cerebral cortex through a hyperpolarization produced by the opening of Cl^- channels (Krnjević, 1984; Alger 1985). Each of these GABA-gated chloride channels is part of a $GABA_A$ receptor complex (Barnard et al., 1987), which is characterized by its sensitivity to the antagonists bicuculline and picrotoxin, and to pharmacological agents, including benzodiazepines and barbiturates (Olsen and Venter, 1986). Other G-protein linked $GABA_B$ receptors (Bowery et al., 1990) are also present in the cerebral cortex (Rakic et al., 1988), but it is the $GABA_A$ receptors that mediate rapid intracortical inhibition (Alger, 1985; Stephenson, 1988; Burt and Kamatchi, 1991).

$GABA_A$ receptors are composed of at least five classes of subunit proteins, designated α, β, γ, δ, and ρ, that differ in their genomic sequences (Fuchs et al., 1988; Khrestchatisky et al., 1989; Schofield, 1989; Shivers et al., 1989; Cutting et al., 1991). The subunit classes include multiple variants ($\alpha 1$–6, $\beta 1$–4, and $\gamma 1$–3) that display considerable sequence homology (Schofield, 1989; Olsen and Tobin, 1990; Seeburg et al., 1990). Coexpression studies have found that each subunit is sensitive to GABA and can form chloride ion channels but that α-, β-, and γ-subunits are required for the expression of a fully functional $GABA_A$ receptor, in which benzodiazepine binding increases the affinity of the receptor for GABA (Levitan et al., 1988a,b; Prichett et al., 1989b; Moss et al., 1991). Presumably, the distribution of

Received May 14, 1993; revised Sept. 29, 1993; accepted Oct. 4, 1993.

This work was supported by Grants EY 06432 (S.H.C.H.) and EY 07193 (E.G.J.) from the National Institutes of Health, U.S. Public Health Service. Human tissue was provided by the University of California, Irvine, National Institute for Mental Health Center for Neuroscience and Schizophrenia (MH44188). We thank Monica Bhandari and Lin Pham for technical assistance.

Correspondence should be addressed to Stewart Hendry, Zanvyl Krieger Mind/Brain Institute, 338 Krieger Hall, Johns Hopkins University, 3400 North Charles Street, Baltimore, MD 21218.

one subunit or of a single variant would follow the distribution of others if a homogeneous population of $GABA_A$ receptors were present in the mammalian cerebral cortex. However, the distribution of neurons in the cerebral cortex and other parts of the CNS expressing mRNAs for a particular subunit of the $GABA_A$ receptor often differs from the pattern displayed for other subunits. In the rodent cerebral cortex the most abundant subunit variants ($\alpha1$, $\beta2$, $\beta3$, and $\gamma2$) are expressed by neurons in the same laminar pattern, but cells expressing other variants ($\alpha2$, $\alpha3$, $\beta1$, and $\gamma1$) are present in different patterns (Wisden et al., 1992). This differential expression of receptor subunits is likely to contribute to a physiological diversity of $GABA_A$ receptor–mediated activities in the CNS (Wisden et al., 1992).

Previous studies of monkey primary visual cortex (area 17) have localized $GABA_A$ receptors principally by the distribution of ^{3}H-muscimol and flunitrazepam binding sites (Shaw and Cynader, 1986; Rakic et al., 1988). In normal monkeys, radioligand binding produces patterns that are similar but not identical to those found with immunocytochemical localization of the $\beta2/3$ subunits (Hendry et al., 1990). These data suggest that subunits of the $GABA_A$ receptor may be differentially localized in monkey area 17. Radioligand binding studies also reveal that $GABA_A$ receptors in human visual cortex are distributed in patterns similar to those in monkey area 17, with highest densities in layers II–III and IVC (Zezula et al., 1988). While these data indicate a basic similarity in the distribution of $GABA_A$ receptors in monkeys and humans, the radioligand binding methods on which they are based are known to obscure details of receptor distribution, such as the prominent density of $GABA_A$ receptors ($\beta2/3$ subunits) detected immunocytochemically in layer IVA of monkeys, their uneven, lattice-like distribution in this layer, and the inhomogeneous, strip-like distribution of these subunits in layer IVC (Hendry et al., 1990). The absence of a high density of binding sites in layer IVA of human visual cortex (Zezula et al., 1988) could arise from similar, technical limitations but may also reflect a difference in organization or neurochemical features. Such differences have been seen previously as an absence of intense cytochrome oxidase (CO) histochemical staining in layer IVA of human visual cortex (Horton and Hedley-White, 1984; Wong-Riley et al., 1993). These questions of differential subunit distribution in monkey visual cortex and possible variation between monkey and human visual cortex were addressed in the present study by examining the distribution of immunocytochemically localized $\alpha1$, $\beta2/3$, and $\gamma2$ subunits in area 17 of normal monkeys and humans.

Ligand-binding and immunocytochemistry demonstrate that the density of $GABA_A$ receptors in adult monkey visual cortex is altered by monocular deprivation. Immunocytochemically detectable levels of the $\beta2/3$ subunits and the binding of radiolabeled muscimol and flunitrazepam are reduced in visual cortical neurons deprived of visual input by intraocular injection of the sodium channel blocker TTX (Hendry et al., 1990). The reductions in receptor levels parallel reductions in GABA- and glutamate decarboxylase (GAD) immunoreactivity in cortical neurons related to the deprived eye (Hendry and Jones, 1986, 1988). Thus, unlike at many synapses in the PNS and CNS, where loss of neurotransmitter leads to compensatory increases in neurotransmitter receptors (Miledi, 1960; Lømo and Rosenthal, 1972; Klein et al., 1989), reductions in GABA in monkey area 17 appear to be accompanied by downregulation of $GABA_A$ receptors. However, the previous study of $GABA_A$ receptor regulation focused on the $\beta2/3$ subunits. Other subunits could remain at normal levels, thus preserving most functional properties of the receptor, or they could display compensatory increases. In the present study, immunocytochemical methods were used to examine the distribution of $\alpha1$, $\beta2/3$, and $\gamma2$ subunits in monocularly deprived monkeys to determine whether each is affected by loss of visual input from one retina. These subunit variants were chosen because they are the most abundant in the mammalian cerebral cortex (Wisden et al., 1992) and, together, form a functional $GABA_A$ receptor (Levitan et al., 1988a; Prichett et al., 1989b; Moss et al., 1991). Our findings indicate the three are similarly distributed in monkey and human visual cortex and that all are regulated by visual activity in adulthood.

Some of these results have been presented in abstract form (Huntsman et al., 1991).

Materials and Methods

Seven adult macaques (*M. mulatta* and *M. fascicularis*), aged 3.5–7.5 years, were used in this study. Two were normal and five were deprived of vision in one eye by the injection of TTX (15 μg/10 μl) into the vitreous body every 5 d for a total of 5, 10, 15, or 30 d. With each injection, the monkeys were anesthetized with ketamine (20 mg/kg, i.m.), after which a topical ophthalmic anesthetic was delivered by placing three or four drops into one eye. Injections of TTX were made through the sclera with a 10 μl Hamilton syringe fitted with a sterile, disposable 30 gauge needle. After the injections were made, a sterile ophthalmic ointment containing bacitracin, neomycin, polymyxin, and 1% hydrocortisone acetate was applied to the cornea and sclera of the injected eye. All monkeys were killed by an overdose of Nembutal (100 mg/kg, i.v.). They were perfused through the heart with 3% or 4% paraformaldehyde in 0.1 M phosphate buffer (pH 7.4). The brains were removed, cut into blocks, and placed in 20% phosphate-buffered sucrose for 3–5 d at 4°C. Most blocks of the occipital lobes were cut so that the lateral surface could be flattened while freezing. Other blocks were cut into 5–10-mm-wide sagittally oriented blocks. All were frozen on dry ice. Sections were cut parallel to the flattened lateral surface or in the sagittal plane, alternating at 20 and 40 μm; the thinner sections were prepared for immunocytochemistry and the thicker for cytochrome oxidase (CO) histochemistry. Selected sections were stained with thionin.

Occipital lobes from three neurologically normal humans (aged 71–79 years) were taken 4–7 hr postmortem, cut into blocks, and fixed by immersion in 4% paraformaldehyde in 0.1 M phosphate buffer overnight at 4°C. The blocks were transferred to 20% phosphate-buffered sucrose and frozen on dry ice. Sections from these blocks were cut in the frontal plane at 40–50 μm and most were reacted in a phosphate-buffered solution of 50% ethanol and 0.3% hydrogen peroxide for 20–30 min at room temperature to eliminate endogenous peroxidase activity. The sections were then washed several times in phosphate buffer and processed for immunocytochemistry (see below). Fixation time and section thickness were greater than those employed in processing monkey tissue because of the much greater fragility of the human postmortem material. A separate series of human sections was reacted for CO in the presence of catalase (Horton and Hedley-White, 1984), and selected sections of human area 17 were mounted and stained with thionin. Some blocks were immersed in fixative for a short time and then dissected to include only upper or lower banks of the calcarine fissure. These were gently flattened between slides and postfixed for several days at 4°C. They were then processed as above.

Sections of both monkey and human cortex were preincubated in dilution buffer (3% normal horse or goat serum and 0.1% Triton X-100 in 0.1 M phosphate buffer) overnight at 4°C and transferred to dilution buffer containing a 1:1000 dilution of rabbit anti-$\alpha1$ antiserum (Benke et al., 1991a), rabbit anti-$\gamma2$ antiserum (Benke et al., 1991b), or mouse anti-$\beta2/3$ antibody (Vitorica et al., 1988). The rabbit antisera were raised against peptides specific for the respective subunits. Their specificity for subunits of the monkey $GABA_A$ receptor was determined by immunoblots of monkey cerebral cortex. Each antiserum reacted with only a single band; that recognized by anti-$\alpha1$ had a molecular weight of 51 kDa, and that recognized by anti-$\gamma2$, a molecular weight of 46–48 kDa. The monoclonal antibody to the $\beta2/3$ subunits recognizes a 57 kDa protein from bovine brain (Vitorica et al., 1988). A previous study

comparing the pattern of immunostaining with this antibody in monkey visual cortex with the pattern produced by binding of ^{3}H-muscimol and ^{3}H-flunitrazepan revealed similar distributions with both methods (Hendry et al., 1990), indicating that the antibody recognizes β2/3 subunits in monkey cortex. Some sections were incubated in anti-γ2 antiserum purified by affinity chromatography over a Sepharose G6 column to which the peptide used for immunization was bound (Benke et al., 1991b). All sections were incubated at 4°C for 24–36 hr, washed, processed by the avidin–biotin–peroxidase method, and reacted in 3,3′-diaminobenzidine and hydrogen peroxide. All sections were mounted on gelatin-subbed slides, dehydrated, and coverslipped.

Selected sections of normal monkey visual cortex were also processed for the simultaneous immunofluorescent detection of two antigens. Three antibody combinations were used: rabbit anti-α1 subunit and mouse anti-β2/3 subunits, mouse anti-β2/3 subunits, and rabbit anti–microtubule-associated proteins (MAPs; ICN, Irvine, CA; diluted 1:4000), and rabbit anti-γ2 subunit and mouse anti-parvalbumin (Sigma Chemical Co., St. Louis, MO; diluted 1:12,000). The anti-MAPs antiserum recognized preferentially the neuronal soma/dendrite-specific MAP 2. For each combination, frozen sections, cut at 10 μm, were preincubated as above and placed in a solution containing both primary antibodies. They were incubated for 12–18 hr at 4°C, washed and processed in a rhodamine-conjugated donkey anti-rabbit IgG (Chemicon, Inc.) and a biotinylated horse anti-mouse IgG (Vector, Inc.) for 1 hr. After further washing, the sections were transferred to a fluorescein isothiocyanate–conjugated streptavidin (Chemicon, Inc.) solution for 1 hr. The sections were mounted onto clean slides, covered in glycerol/phosphate buffer, examined, and photographed under epifluorescence with rhodamine and fluorescein filter cubes.

Control experiments involved the replacement of the specific anti-α1 or γ2 antisera or anti-β2/3 monoclonal antibody with nonimmune rabbit serum or nonimmune mouse serum. For the immunofluorescence experiments, the anti-γ2, -α1, and -MAPs antisera were replaced with nonimmune rabbit serum, the anti-β2/3 with normal mouse serum and the anti-parvalbumin with antibody adsorbed with 10 μM parvalbumin conjugated to polyacrylamide (Sigma Chemical Co). Each of these replacement or adsorption procedures eliminated the specific immunostaining and left a very light diffuse reaction.

Results

$GABA_A$ receptor subunit distribution in normal monkey area 17

Laminar distribution. Immunoreactivity for the α1, β2/3, and γ2 subunits of the receptor was unevenly distributed in monkey area 17 (Fig. 1). Immunoreactivity for α1 was present in all layers but was most intense in three wide bands, which included layers II–III, IVCβ, and VI, and in an additional, very narrow band, restricted to layer IVA (Fig. 1*B*). Immunoreactivity for β2/3 was similarly distributed, with intense immunostaining in layers II–III, IVA, and VI and greater immunostaining in layer IVCβ than in layer IVCα (Fig. 1*C*). Immunoreactivity for γ2 was also relatively intense in layer IVC; the difference between IVCα and IVCβ was less than that detected for the other subunits. A moderately intense, thin band was present in layer IVA but the immunostaining in that layer, in layers II and III and in layer VI was less than that seen for the α1 and β2/3 subunits (Fig. 1*D*). For all three subunits, layers I, IVB, and V contained light to moderate immunostaining.

Immunoreactivity for the α1 and β2/3 subunits was located in the neuropil of each layer, such that the somata and large dendrites of neurons were conspicuous as unstained regions (Figs. 2, 3). The immunostained neuropil frequently occurred in small clusters, especially in layer IVC (Fig. 2*A,B*) and the staining for each subunit appeared punctate or formed thin rims around circular unstained regions (Fig. 2*C*). Direct comparison of immunostaining for β2/3 subunits with that for MAPs demonstrated that the receptor immunoreactivity was absent from the somata and large primary dendrites of cortical neurons (Fig. 3*A–D*). Instead, intense receptor immunostaining was found in regions that contained radial bundles of dendrites (Fig. 3*A,B,E,F*) or in clusters that contained high densities of thin dendritic segments (Fig. 3*C–F*). As with immunoperoxidase-based localization methods, the immunofluorescent methods revealed evidence of thin rims of receptor subunit immunostaining apposed to the somata and large primary dendrites of cortical neurons (Fig. 3*A–D*).

With antibodies to α1 and β2/3 subunits, few cells, present only at the border between layer VI and the white matter, displayed cytoplasmic immunoreactivity (Fig. 4). This immunostaining filled the somata and long processes of these cells (Fig. 4*A*), which often formed elaborate plexuses (Fig. 4*B*). Because of their sizes and morphologies, we considered it most likely these cells were neurons, but to determine their identity conclusively we compared immunoreactivity for β2/3 subunits with that for MAPs. All cells immunostained for β2/3 subunits in the white matter were also immunostained for MAPs (Fig. 4*C,D*), demonstrating they were neurons.

Much of the γ2 immunoreactivity was also located in the neuropil, in which fine punctate profiles were stained. In addition, numerous somata through the thickness of area 17 displayed intense cell surface immunostaining with both the nonpurified and the affinity-purified anti-γ2 antisera (Fig. 5). Most of the surface-immunostained neurons occupied layers I–IVCα but some were present in layers IVCβ–VI (Fig. 5*A,B*). This immunostaining appeared as a surface matrix of intensely immunoreactive material that surrounded unstained punctate zones, 1–2 μm in diameter (Fig. 5*C*). The matrix covered the surfaces of somata and primary dendrites of cells that resembled nonpyramidal neurons, by both the round or oblong shape of the somata and the absence of prominent apical dendrites (Fig. 5*C*). The surface-immunostained cells were conclusively identified as nonpyramidal cells and were classified as a subpopulation of GABA neurons in experiments where γ2 receptor immunofluorescence was localized simultaneously with immunofluorescence for parvalbumin (Fig. 5*D–G*), a protein that coexists with GABA in neurons of monkey area 17 (Hendry et al., 1989; Van Brederode et al., 1990). All neurons with γ2 surface immunostaining were also parvalbumin immunoreactive (Fig. 5*D–G*), yet some parvalbumin-positive somata in all layers of area 17 displayed no γ2 surface immunostaining.

Compartmental distribution. Intense immunoreactivity for the β2/3 subunits occupied the regions of the CO-rich puffs in layers II–III (Fig. 6*C*; see also Hendry et al., 1990). A similar pattern of immunoreactivity for the α1 and γ2 subunits was also detected, as periodic patches of relatively intense α1 and γ2 immunostaining lined up in rows through layers II and III (Fig. 6*B,D*). These patches were as robust as those immunostained for β2/3 and were similar in size (approximately 80 × 120 μm) and in their distribution in rows. Comparison of the immunostaining for α1, β2/3, or γ2 with the histochemical staining for CO (Fig. 6*A*) showed that each immunostained patch in layers II and III corresponded to a CO puff. Immunostaining for α1, β2/3, and γ2 subunits was uniform in layers IVB, V, and VI, with no evidence of immunostained patches, even though these layers also contain CO puffs.

Immunostaining for the β2/3 subunits in layer IVA consists of an intense lattice (Fig. 7*B,E*), which was found previously to correspond to the walls of the CO-stained honeycomb in that layer (Hendry et al., 1990). A similar immunostained lattice was detected with localization of both the α1 (Fig. 7*A,D*) and γ2

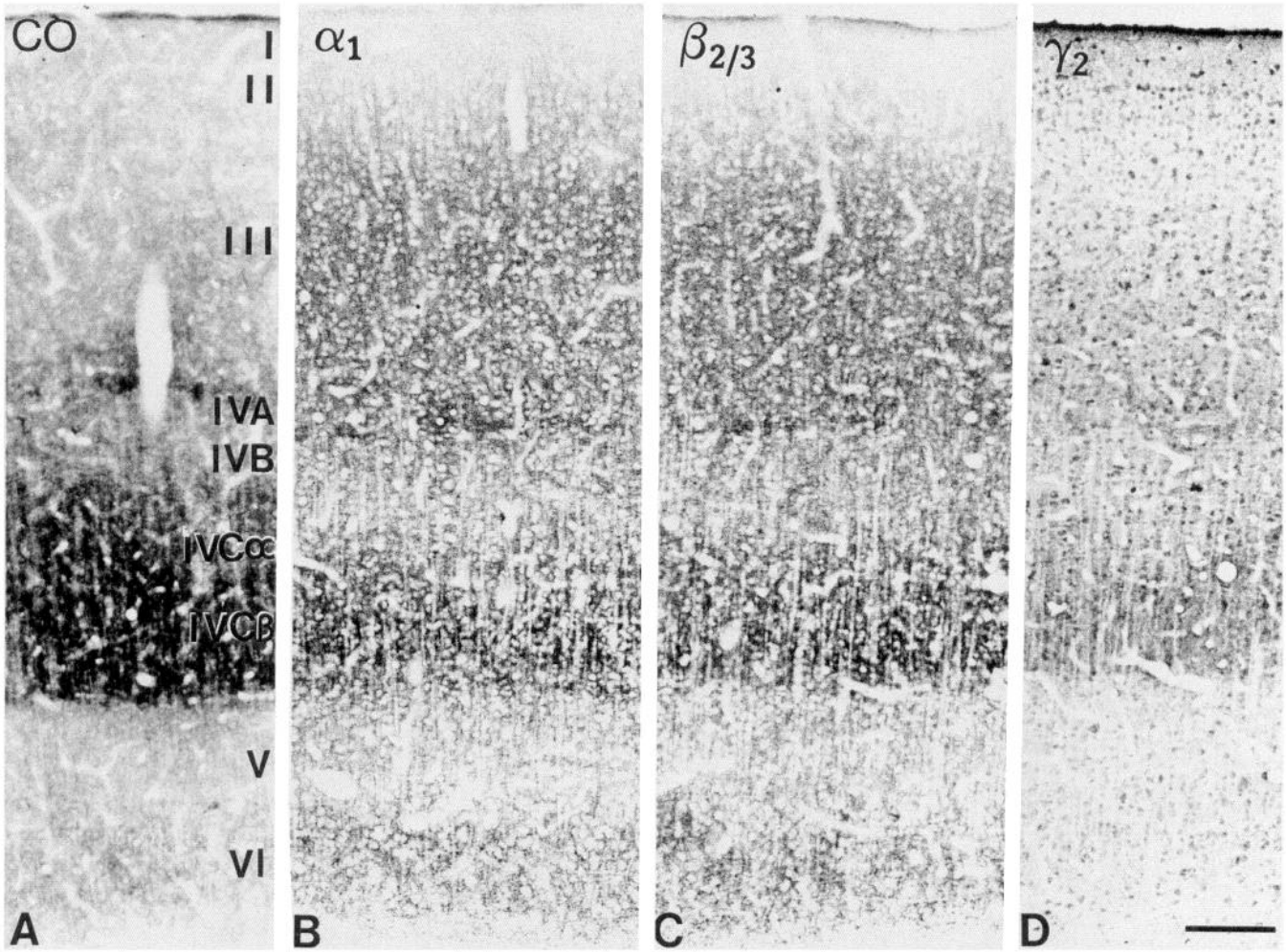

Figure 1. Laminar distribution of $GABA_A$ receptor subunit immunoreactivity in normal monkey visual cortex. *A*, Section stained histochemically for CO. The characteristic pattern of staining was used to determine the laminar borders in adjacent immunostained sections. *B*, The distribution of $\alpha 1$ immunoreactivity. Relatively intense immunostaining occupies layers II–III, IVC, particularly IVCβ, and VI. A thin band of intense but interrupted immunostaining beneath layers II–III corresponds to layer IVA. *C*, The distribution of $\beta 2/3$ immunostaining. The pattern is similar to that seen for $\alpha 1$, except for a slightly greater immunostaining of layer IVCβ. *D*, The distribution of $\gamma 2$ immunostaining. In addition to lighter immunostaining of layers II–III and VI, $\gamma 2$ immunoreactivity differs from that of $\beta 2/3$ in displaying less of a difference between layers IVCα and IVCβ. Immunoreactivity in layer IVA is also relatively difficult to detect in sections cut along radial lines (compare with Fig. 7*C*). Numerous darkly immunostained cells are apparent in the section. Scale bar, 250 μm.

subunits (Fig. 7*C*). As with immunoreactivity for the $\beta 2/3$ subunits, immunoreactivity for the $\alpha 1$ and $\gamma 2$ subunits in layer IVA included thin walls, approximately 20 μm thick, in which the staining was relatively intense. These walls were seen in tangentially cut sections to surround lightly immunostained, circular or oblong regions, 40–120 μm in diameter (Fig. 7*D*). Within both the walls of the lattice and the central, lightly stained regions were numerous unstained neuronal somata (Fig. 7*D,E*).

In layer IVC, immunoreactivity for all the subunits appeared uniform at low magnification, with no evidence of periodic patches or stripes. However, at high magnification a lattice of immunoreactivity was detected for each subunit (Fig. 2). This lattice had an irregular pattern in which thin walls of intense immunoreactivity surrounded lighter stained regions that contained a relatively pale neuropil and two or three unstained somata. Because of the similarity in subunit distribution in layers IVA and IVC, particularly the presence of all three within the thin latticework of layers IVA and IVC, coexistence of subunits appeared likely. Direct comparison of $\alpha 1$ and $\beta 2/3$ distribution in these layers showed the two to occupy the same locations (Fig. 8). Even at the highest magnifications, immunostaining for both subunits overlapped completely.

Distribution in human area 17

The pattern of $GABA_A$ receptor subunit immunoreactivity localized in area 17 of humans was similar to that seen in area 17 of macaques. In frontal sections through the human visual cortex, intense immunoreactivity for all three subunits was present in layer IVC and, to a lesser extent, in layers II–III and VI (Fig. 9). Immunoreactivity for all three subunits appeared more intense in layer IVCβ than in IVCα, although this difference was particularly obvious for the $\beta 2/3$ subunits (Fig. 9*C*). Immunoreactivity for $\alpha 1$ (Fig. 9*B*) and $\gamma 2$ (Fig. 9*D*) appeared more even in intensity through the depth of this layer. For all subunits, but especially the $\beta 2/3$ subunits, a thin, relatively intensely immunostained band was also present in layer IVA (Fig. 9*C*).

As in the white matter beneath monkey area 17, neurons subjacent to human area 17 displayed cytoplasmic immuno-

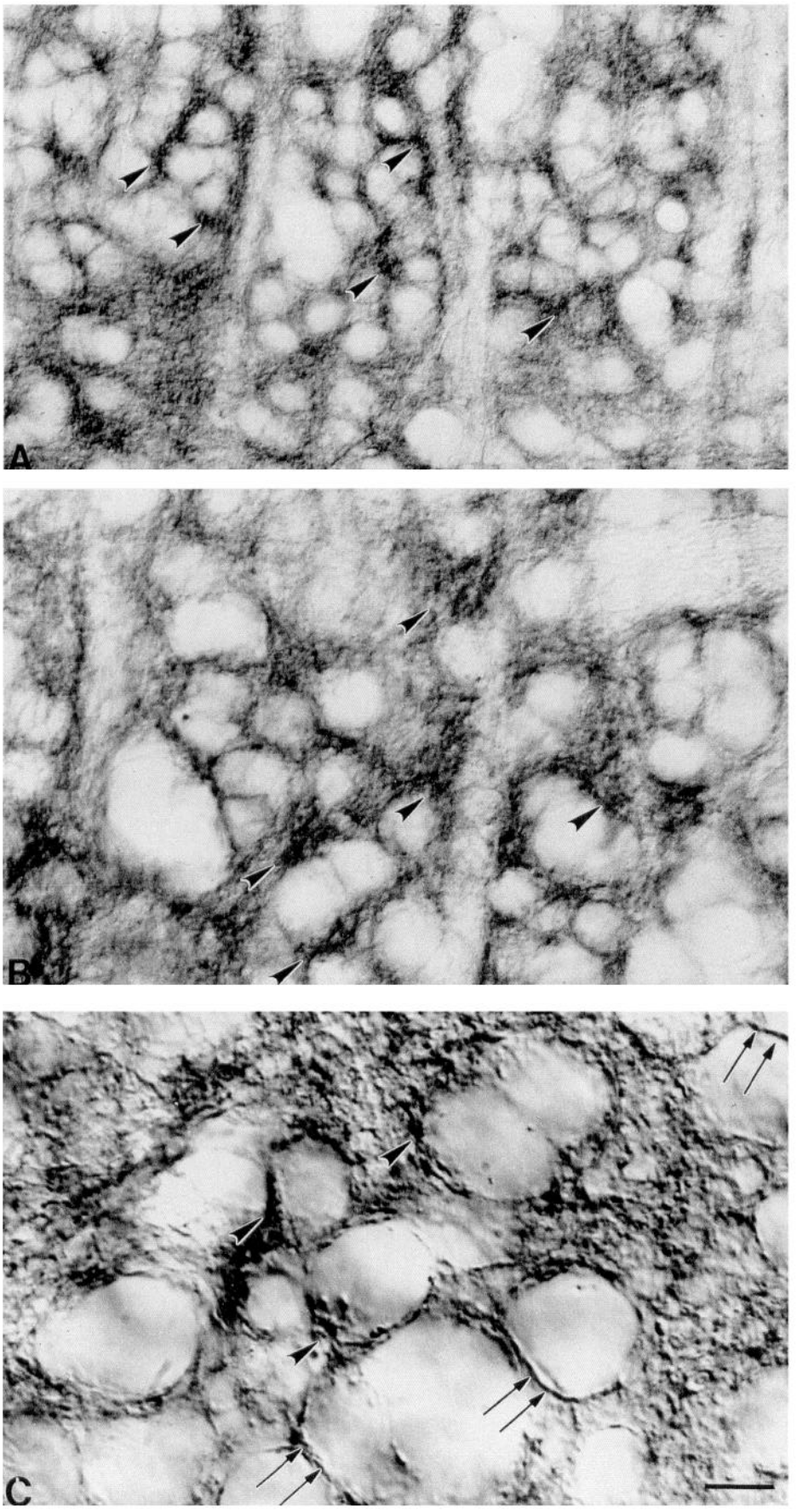

Figure 2. Details of α1 and β2/3 immunoreactivity in sagittal sections through monkey visual cortex. *A* and *B*, Clusters of α1 (*A*) and β2/3 (*B*) immunostaining, some of which are designated by *arrowheads*, occupy layer IV$C\beta$. These clusters vary in size and are separated from one another by circular unstained regions and narrow, radially oriented zones. *C*, Differential interference contrast photomicrograph of β2/3 immunostaining in layer III. Discrete immunostained puncta are scattered throughout this region (*arrowheads*) and, in addition, thin immunostained zones (*double arrows*) outline the peripheries of circular unstained regions. Scale bar: 35 μm for *A*, 20 μm for *B*, 15 μm for *C*.

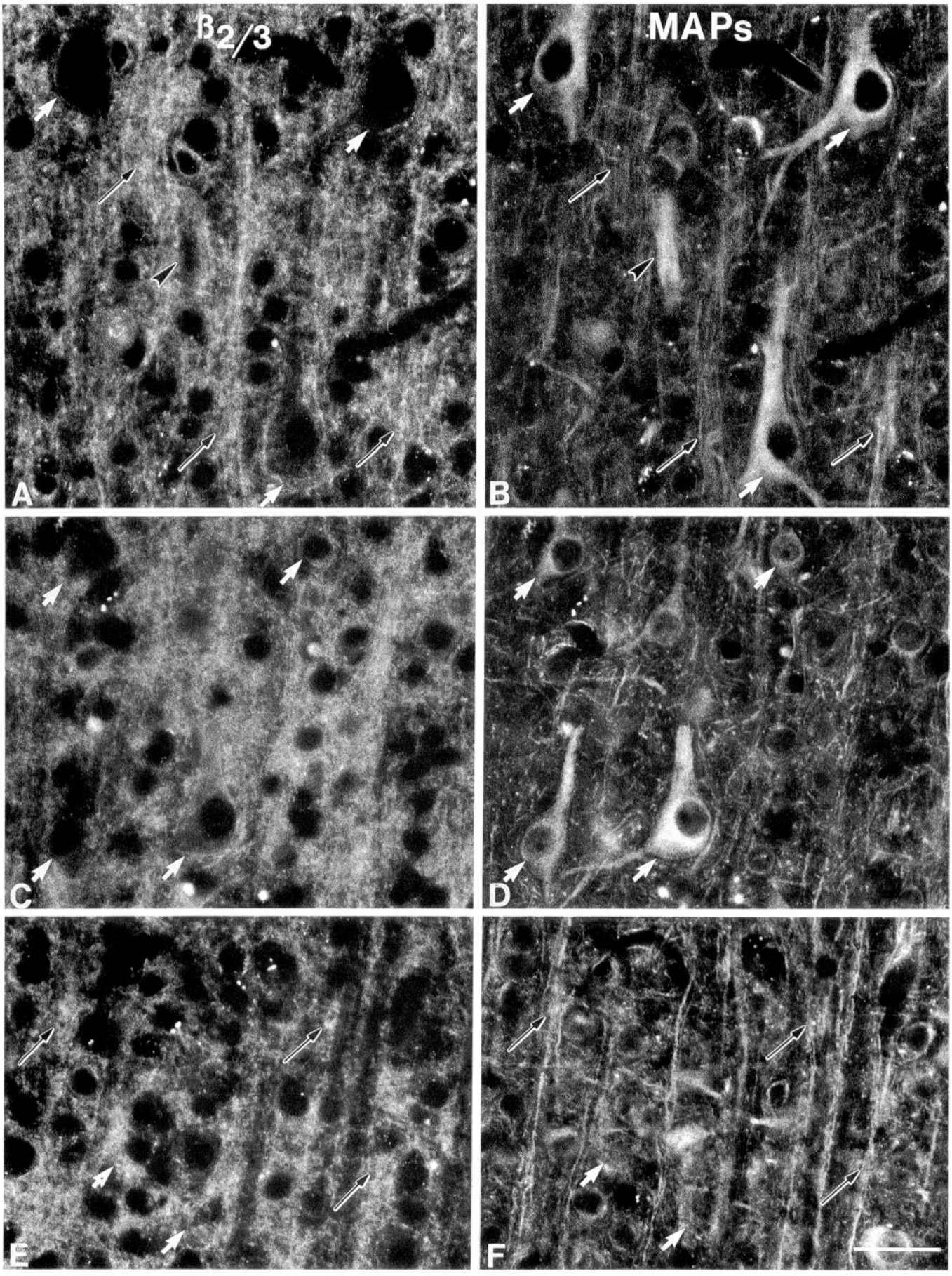
ß2/3
MAPs
A
B
C
D
E
F

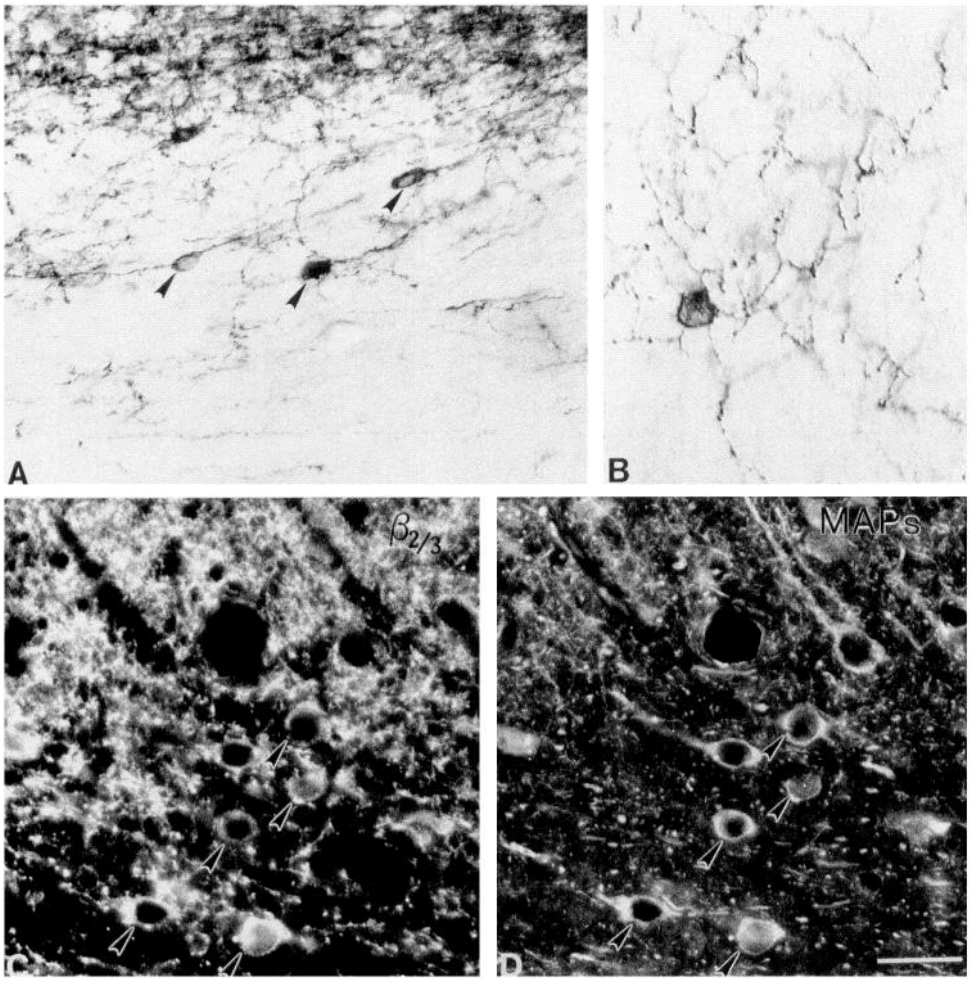

Figure 4. Immunostaining of neurons in the white matter beneath monkey area 17. *A*, Photomicrograph of immunoreactivity for $\alpha 1$ subunit in the white matter subjacent to area 17. The somata and processes of several cells (*arrowheads*) are immunostained for this subunit. *B*, Differential interference contrast micrograph of an $\alpha 1$ immunostained cell 400 μm deep to the border between layer VI and the white matter. A dense plexus of immunostained processes occupies the region near the immunostained soma. *C* and *D*, Pair of fluorescence photomicrographs immunostained for $\alpha 1$ (*C*) and MAPs (*D*). Cells in the white matter showing cytoplasmic immunostaining for $\alpha 1$ are also MAP immunoreactive (*arrowheads*), demonstrating that these are neurons. Scale bar: 75 μm for *A*, 40 μm for *B–D*.

staining of somata and processes (Fig. 10*B*). These neurons resembled closely the cells in the white matter beneath monkey cortex. Also, as in the monkey, immunoreactivity for the $\gamma 2$ subunit included not only punctate profiles in the neuropil but also a matrix on the surfaces of some neurons (Fig. 10*A*). These cells were most commonly found in layers II–IVB.

An uneven distribution of receptor immunostaining characterized layer IVC of the human visual cortex and was particularly evident with localization of $\beta 2/3$ subunits (Figs. 9*C*, 11*A*). Immunostaining for those subunits consisted of thin, radially oriented stripes of intensely immunoreactive processes, 20–30 μm wide, separated by wider stripes (30–60 μm wide) in which the immunostaining was extremely light. The width of the intensely immunostained stripes was greatest in the deepest part of layer IVCβ, where the width of the lightly stained stripes was correspondingly least. Yet at progressively more superficial locations in this layer, the intensely immunostained stripes narrowed and the lightly stained stripes between them widened (Fig. 11*A*). This change in pattern was obvious in tangential sections through layer IVCβ. At its superficial extreme, the intensely immunostained stripes appeared as a loosely organized lattice that surrounded a series of circular or oblong, lightly immunostained zones (Fig. 11*D*). This region appeared very similar to layer IVA of monkey area 17 (compare Figs. 7*A–C*, 11*D*). Only 160 μm deeper in layer IVC, the $\beta 2/3$ immunostaining appeared as a much more tightly organized lattice, in which intensely immunostained clusters surrounded small, lightly immunostained regions (Fig. 11*E*).

In sections cut along radial lines, the immunostained stripes of layer IVCβ extended into layer IVCα and continued through layer IVB, into layer IVA of human area 17 (Fig. 9*C*). Tangential sections through layers IVCα and IVA displayed evidence of uneven staining yet the immunoreactivity was insufficiently intense to determine if it formed a lattice. Similarly, the immu-

←

Figure 3. Comparison of immunostaining for $\beta 2/3$ subunits and microtubule-associated proteins (*MAPs*) in monkey area 17. *A* and *B*, Pair of fluorescent photomicrographs from layer III showing the immunostaining for $\beta 2/3$ (*A*) and MAPs (*B*). The somata of large neurons (*white arrows*) and a large radially oriented dendrite (*arrowheads*) are surrounded by $\beta 2/3$-immunoreactive elements but are, themselves, unstained. The most intense $\beta 2/3$ immunostaining is present in regions that contain bundles of thin MAP-immunoreactive dendrites (*black arrows*). *C* and *D*, Pair of fluorescent photomicrographs from layer IVB. MAP-immunostained somata (*arrows*) are not immunoreactive for $\beta 2/3$, but the largest one is outlined by immunoreactive elements. Although this layer is more lightly immunostained for $\beta 2/3$ than adjacent layers, its most intense $\beta 2/3$ immunostaining is present in regions that contain small dendritic fragments. *E* and *F*, Pair of fluorescent photomicrographs from layer VI. Clusters of intense $\beta 2/3$ immunoreactivity are present in regions that contain short dendritic segments (*white arrows*) or bundles of radially oriented dendrites (*black arrows*). Scale bar, 35 μm.

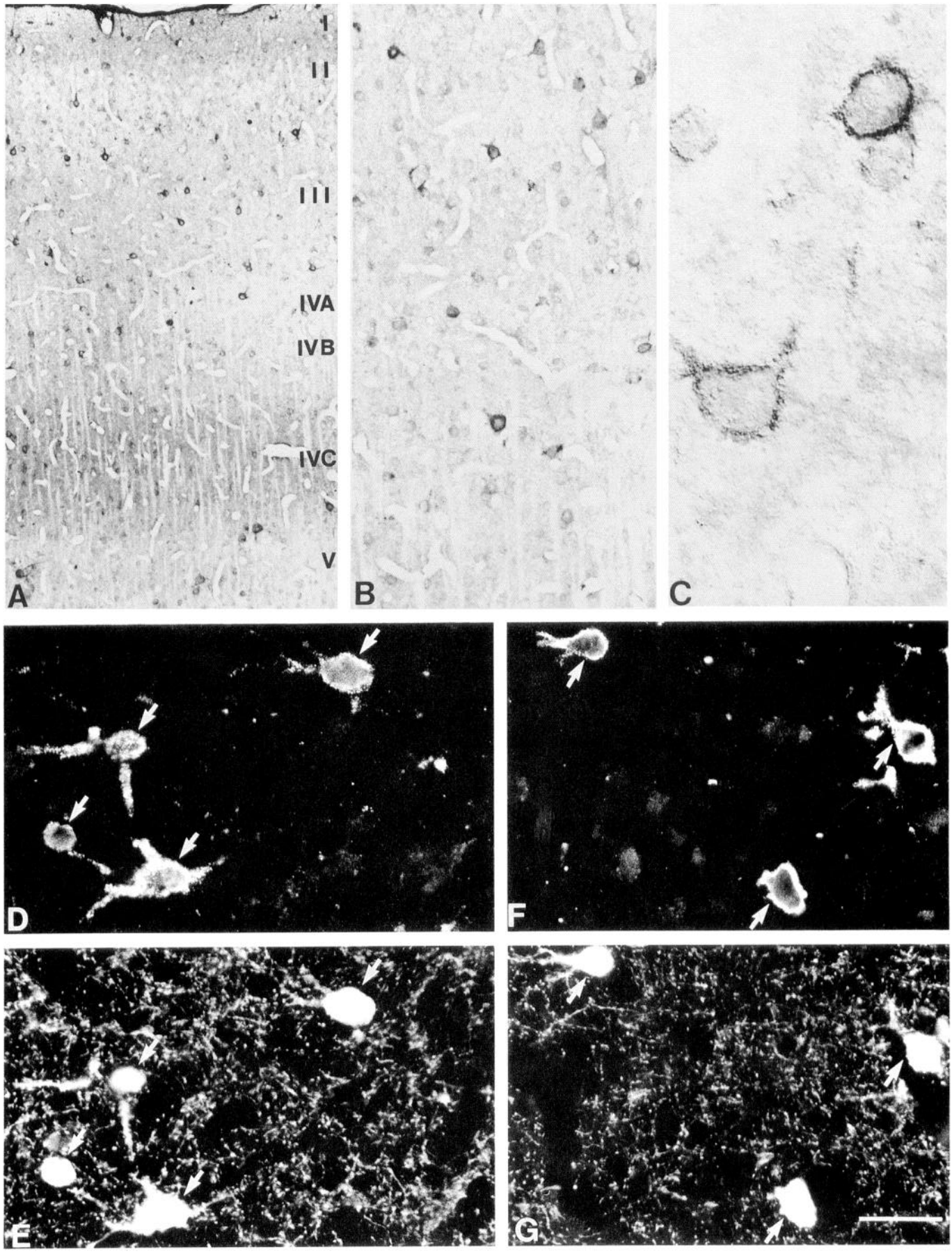
I
II
III
IVA
IVB
IVC
V
A
B
C
D
F
E
G

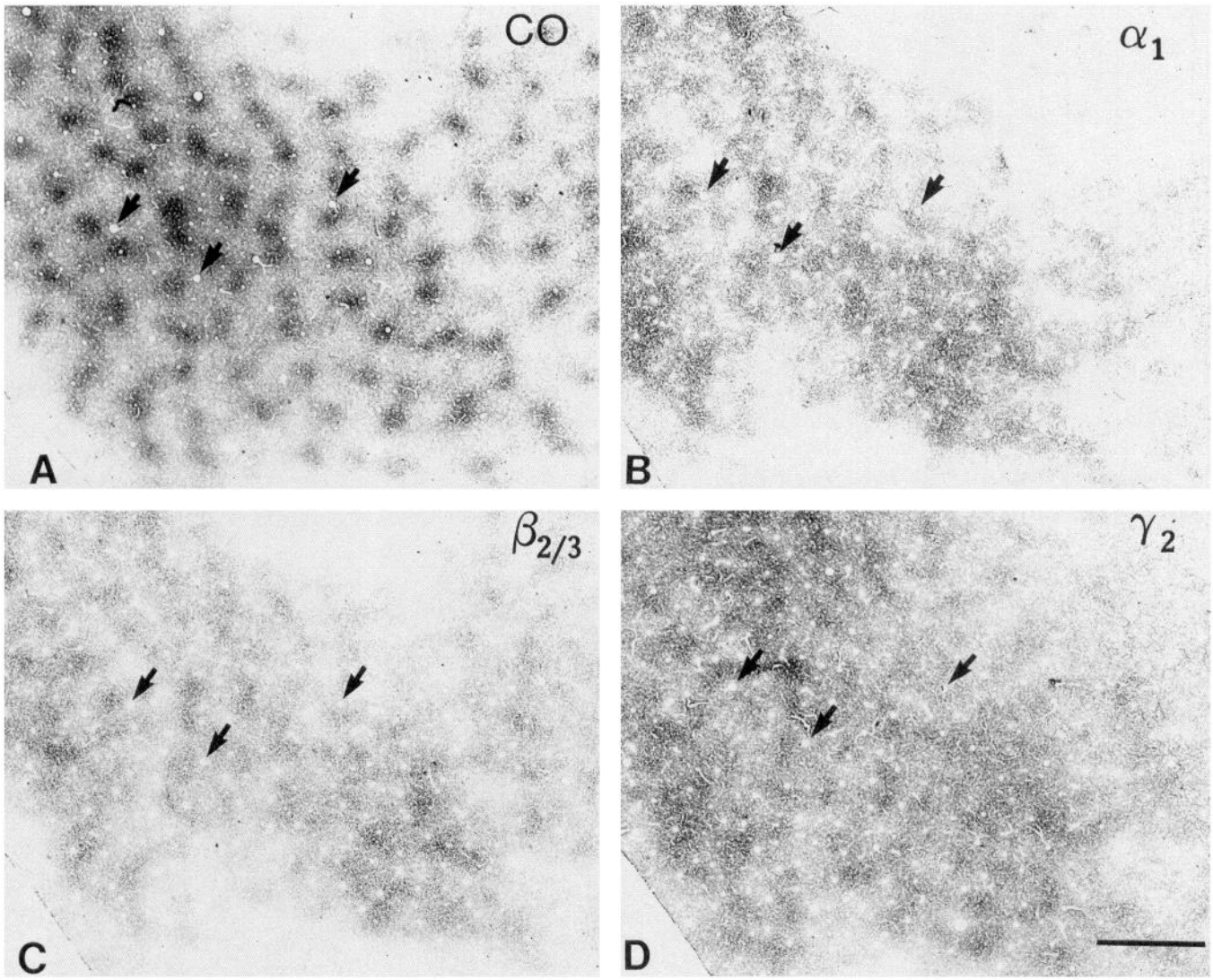

Figure 6. Patchy distribution of receptor subunit immunoreactivity in layers II and III of monkey area 17. *A*, Photomicrograph of a tangential section through layers II and III stained histochemically for CO. Intensely stained CO puffs form elongated rows. *B–D*, Photomicrographs of sections adjacent to A immunostained for α1 (*B*), β2/3 (*C*), and γ2 (*D*). In sections immunostained for each subunit, periodic patches of intense immunoreactivity line up in rows. By comparing the positions of the same blood vessel profiles in these sections (*arrows*), the patches of α1, β2/3, and γ2 immunostaining are found to coincide with the puffs of intense CO staining. Scale bar, 700 μm.

nostaining of layers II and III was too light to determine if patches of receptor immunoreactivity existed. This failure to produce intense immunostaining in tangential sections through layers that were well stained in frontal sections is most likely related to the flattening procedure and prolonged aldehyde fixation that accompanied it.

Surrounded by the intensely immunostained lattice in both superficial and deep layer IVCβ were numerous unstained circular regions (Fig. 11*B*), which appeared to be neuronal somata. The pattern was typical of the neuropil immunostaining in all layers of human visual cortex and consisted of punctate zones that varied in size and in intensity of immunostaining (Fig. 11*C*).

Deprivation-induced changes in receptor immunostaining

The distribution of immunoreactivity for the α1, β2/3, and γ2 subunits in layer IVC of monkey area 17 changed following the elimination of ganglion cell activity in one retina: instead of

←

Figure 5. Immunostaining for γ2 subunit in monkey visual cortex. *A*, Photomicrograph of a section immunostained with the unpurified anti-γ2 antiserum, showing the distribution of somata displaying intense cell-surface immunoreactivity. The immunostained somata are present through the full thickness of area 17. *B*, Photomicrograph of a section immunostained with affinity-purified anti-γ2 antiserum. Numerous somata displaying cell-surface immunostaining are present. *C*, Differential interference contrast photomicrograph, showing details of the cell-surface immunostaining. The scalloped appearance of the reaction product is evident on the surfaces of two intensely immunostained somata. *D–G*, Pairs of fluorescence photomicrographs of γ2 (*D* and *F*) and parvalbumin (*E* and *G*) immunoreactivity in layers III (*D* and *E*) and V (*F* and *G*) of monkey visual cortex. Individual somata (*arrows*) that display intense cell-surface immunostaining for γ2 are also parvalbumin immunoreactive, indicating they are GABAergic neurons. Scale bar: 350 μm for *A*, 170 μm for *B*, 20 μm for *C*, 45 μm for *D–G*.

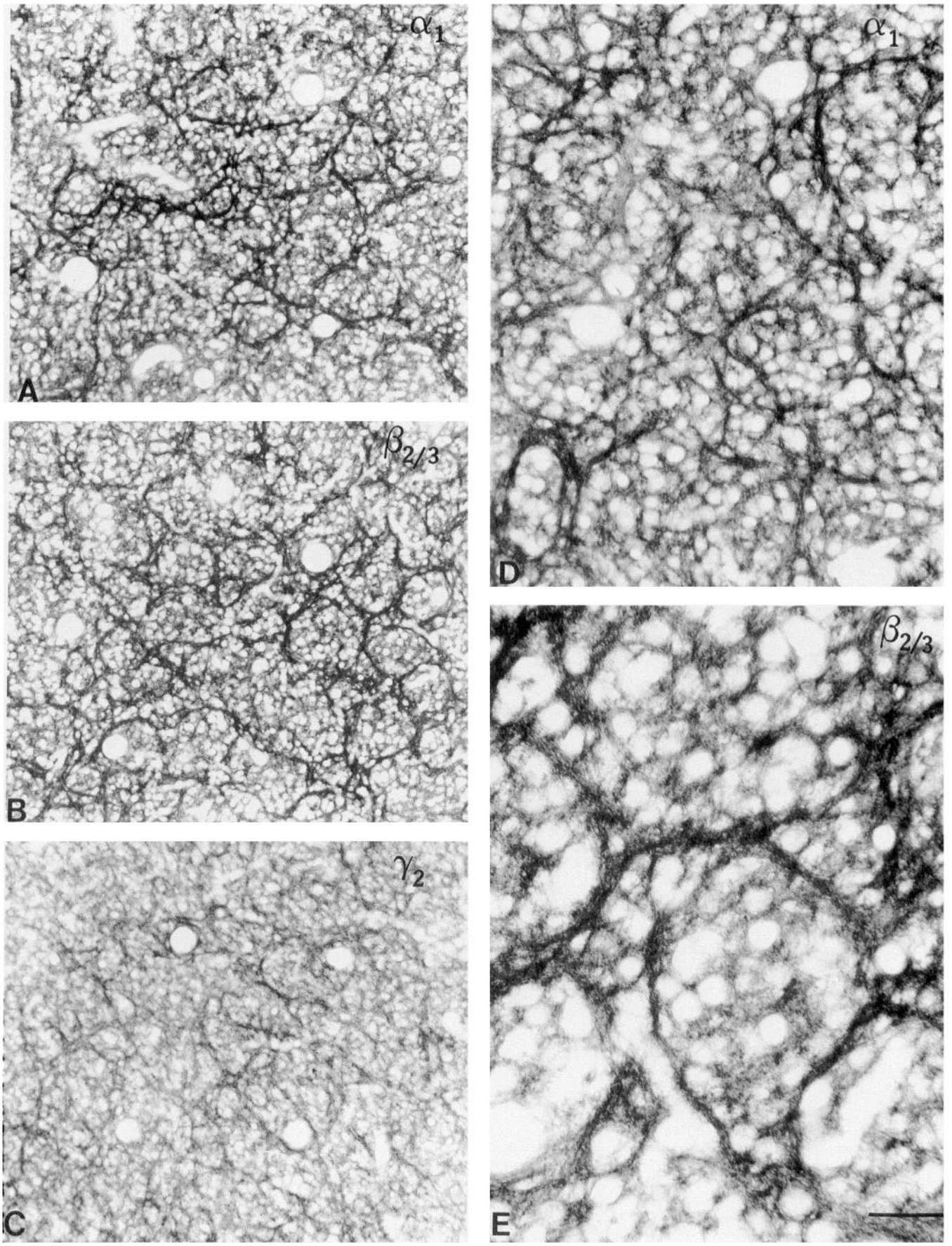
α_1
A
$\beta_{2/3}$
B
γ_2
C
α_1
D
$\beta_{2/3}$
E

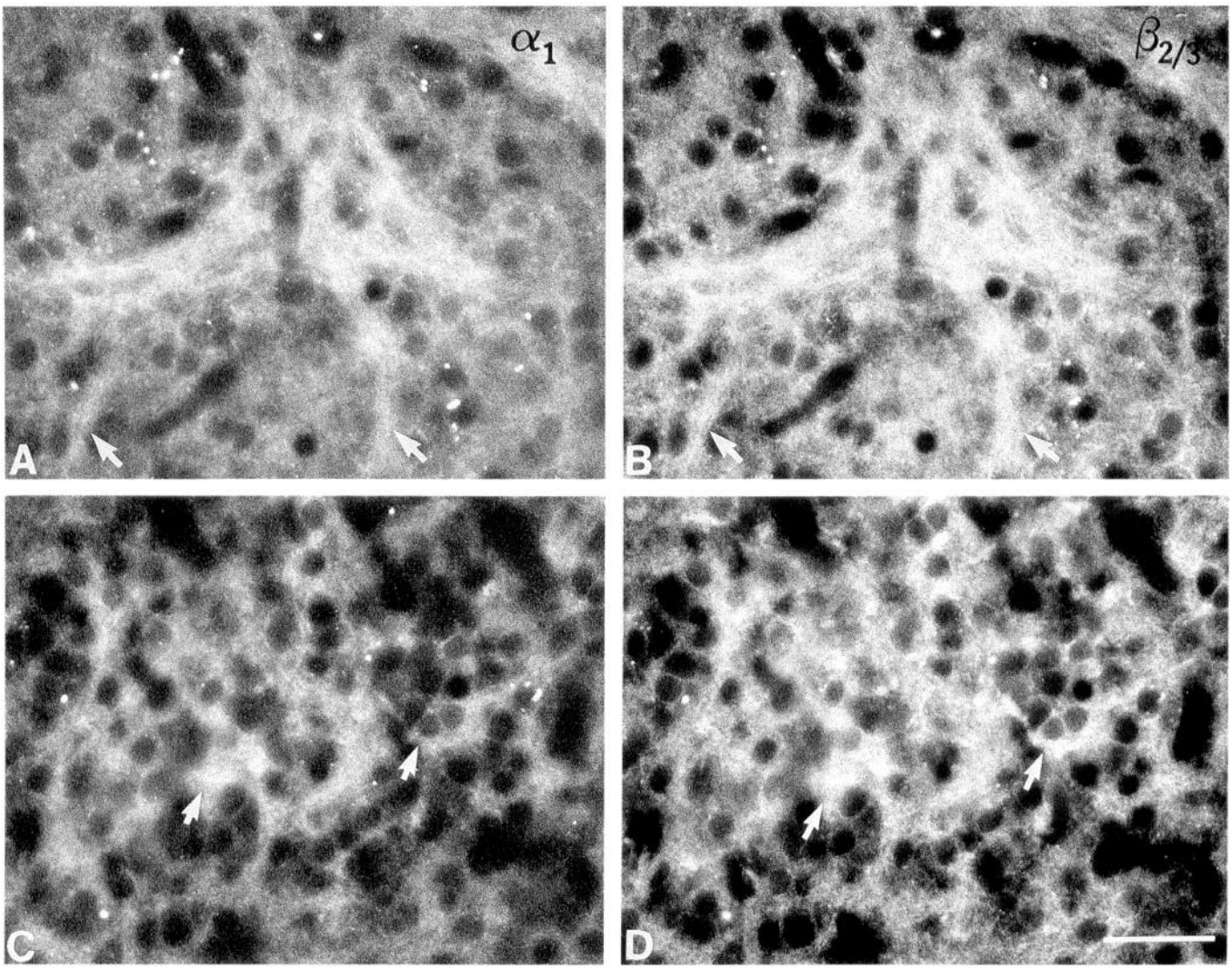

Figure 8. Colocalization of $\alpha 1$ and $\beta 2/3$ subunits in layer IV of monkey visual cortex. *A* and *B*, Simultaneous immunofluorescent detection of $\alpha 1$ (*A*) and $\beta 2/3$ (*B*) subunits in layer IVA, using rabbit anti-$\alpha 1$ and mouse anti-$\beta 2/3$ antibodies. Intense immunoreactivity for these subunits is present in the same regions, including a central cluster and thin arms of a lattice (*arrows*). *C* and *D*, Localization of $\alpha 1$ (*C*) and $\beta 2/3$ (*D*) in layer IVCβ. Clusters of intense immunoreactivity, two of which are indicated by *arrows*, make up the immunostaining patterns for these subunits in layer IVCβ. The same regions, which include punctate zones of immunoreactivity, are immunostained with the two antibodies. Scale bar, 50 μm.

homogeneously intense immunoreactivity, the pattern of localization for each subunit became one of alternating lightly and intensely immunostained stripes, each 300–500 μm wide (Figs. 12, 13). Comparison with adjacent sections histochemically stained for CO showed that the lightly immunostained stripes corresponded to the lightly CO-stained stripes (deprived-eye stripes) and darkly immunostained stripes corresponded to darkly CO-stained stripes (normal-eye stripes). The same pattern was found in both layer IVCα and layer IVCβ with alternating stripes of intense and light immunostaining detected in both sublaminae, corresponding to alternating stripes of intense and light CO staining. Simultaneous processing of sections through area 17 from normal and monocularly deprived monkeys produced immunostaining in layer IVC of the normal monkey that was similar in intensity to the immunostaining of normal-eye columns and was markedly greater than the immunostaining of deprived-eye columns in the TTX-injected monkeys.

The time course of the changes in receptor subunit immunostaining was determined by examining sections from monkeys monocularly deprived for 5–30 d. At the earliest survival time, stripes, lightly and intensely immunostained for $\alpha 1$, $\beta 2/3$, and $\gamma 2$ subunits were evident in layer IVC (Fig. 12). The stripes

←

Figure 7. Receptor subunit immunostaining in layer IVA of monkey visual cortex. *A–C*, Photomicrographs of tangential sections from the same monkey immunostained for $\alpha 1$ (*A*), $\beta 2/3$ (*B*), and $\gamma 2$ (*C*). For each subunit, a lattice, composed of intensely immunostained walls, surrounds more lightly immunostained central regions. The intensely stained walls surround regions that vary in width from 40 to 120 μm in diameter. The lattice walls are more intensely immunostained for $\alpha 1$ and $\beta 2/3$ than $\gamma 2$. *D* and *E*, High-magnification photomicrographs of $\alpha 1$ (*D*) and $\beta 2/3$ (*E*) immunostaining. With both subunits, the intensely immunostained lattice walls surround regions that contain circular unstained regions, which we interpret as the somata of unstained neurons. Scale bar: 200 μm for *A–C*, 100 μm for *D*, 50 μm for *E*.

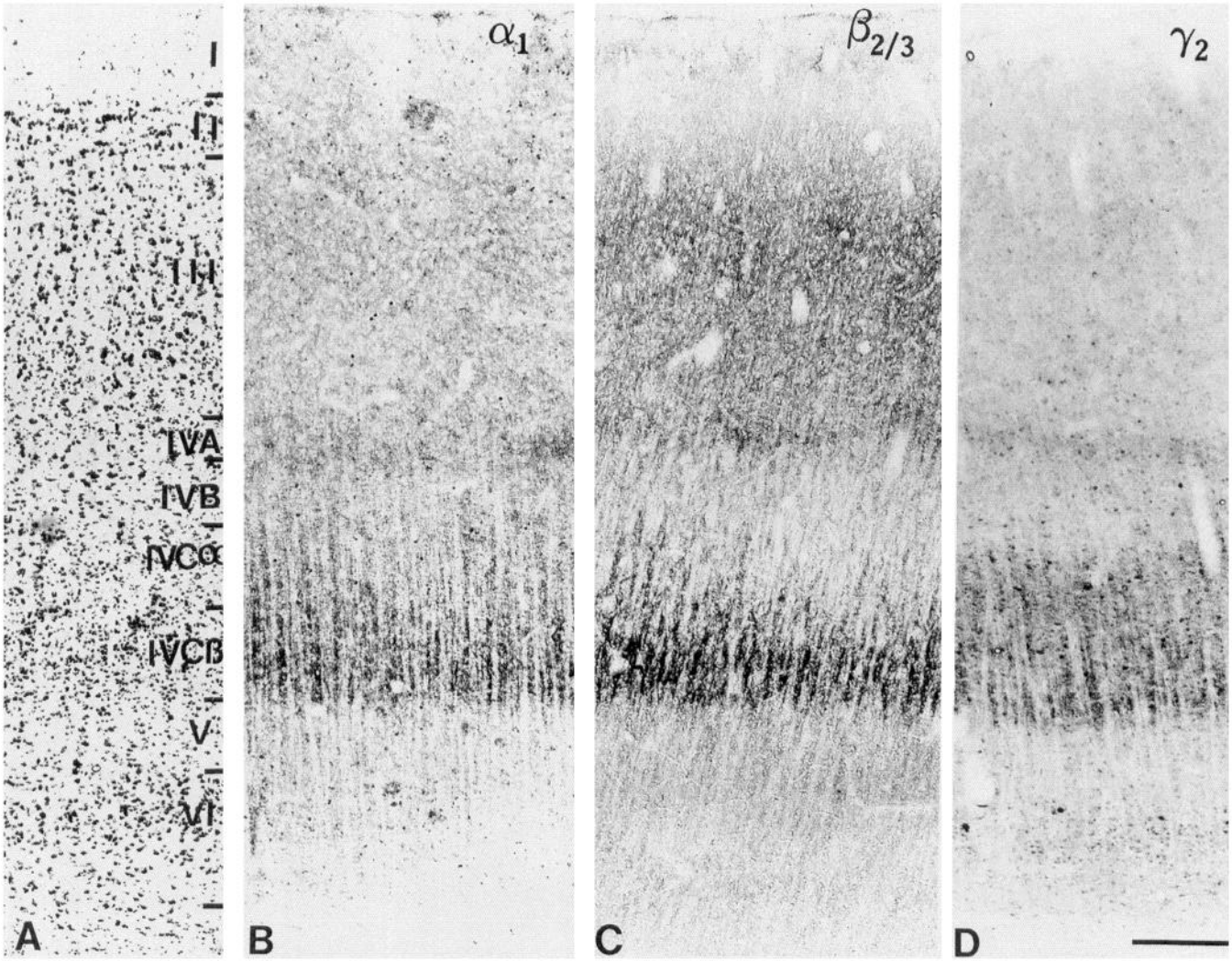

Figure 9. Distribution of $GABA_A$ receptor subunit immunostaining in normal human visual cortex. *A*, Photomicrograph of a section stained with thionin. The relative size and density of neurons were used to divide area 17 into six layers (*I–VI*) and to subdivide layer IV into four sublaminae. *B–D*, Photomicrographs of adjacent sections immunostained for $\alpha 1$ (*B*), $\beta 2/3$ (*C*), and $\gamma 2$ (*D*). All are most intensely immunostained in layer IVC, particularly in layer IVCβ. Enhanced immunostaining is present in layer IVA in sections processed for each of the subunits and especially for $\beta 2/3$ (*C*). Scale bar, 250 μm.

persisted through the intermediate survival periods and were still apparent in sections immunostained for each subunit after 30 d of monocular deprivation (Fig. 13).

The lighter immunostaining in layer IVC of stripes related to the TTX-injected eye appeared as a general reduction in the intensity of neuropil immunoreactivity for each of the three subunits. Because the neuropil immunostaining was diffusely distributed as very small puncta (see above) it could not be determined whether the reduced immunostaining represented a reduction in the number or in the intensity of immunostained elements. For the $\gamma 2$ subunit, the reduction in immunostaining was found only in the neuropil and did not appear to involve changes in the intense immunoreactivity along the surfaces of neurons in layer IVC.

Discussion

$GABA_A$ receptors are the principal mediators of synaptic inhibition in the mammalian CNS. They are the sites at which several pharmacological agents and, putatively, several endogenous compounds operate, including not only GABA and its agonists but also benzodiazepines, barbiturates, alcohol, and steroids (Stephenson, 1988; Sieghart, 1989; Olsen and Tobin, 1990; Burt and Kamatchi, 1991). $GABA_A$ receptors are thought to resemble other members of the ligand-gated ion channel family in their composition of five subunit proteins surrounding a central ion channel (Olsen and Venter, 1986; Burt and Kamatchi, 1991; Lüddens and Wisden, 1991). The wide diversity of $GABA_A$ subunit variants makes it possible for some 200,000 combinations to exist in the mammalian CNS, yet it is likely that fewer than 100 are actually assembled into functional receptors by mammalian neurons (Burt and Kamatchi, 1991). These combinations differ from one another in their response to the release of GABA or the administration of pharmacological agents (Sieghart, 1989; Sigel et al., 1990; Burt and Kamatchi, 1991).

The principal observations of the present study are that three major subunit variants of the $GABA_A$ receptor are distributed in very similar patterns within monkey area 17, that their dis-

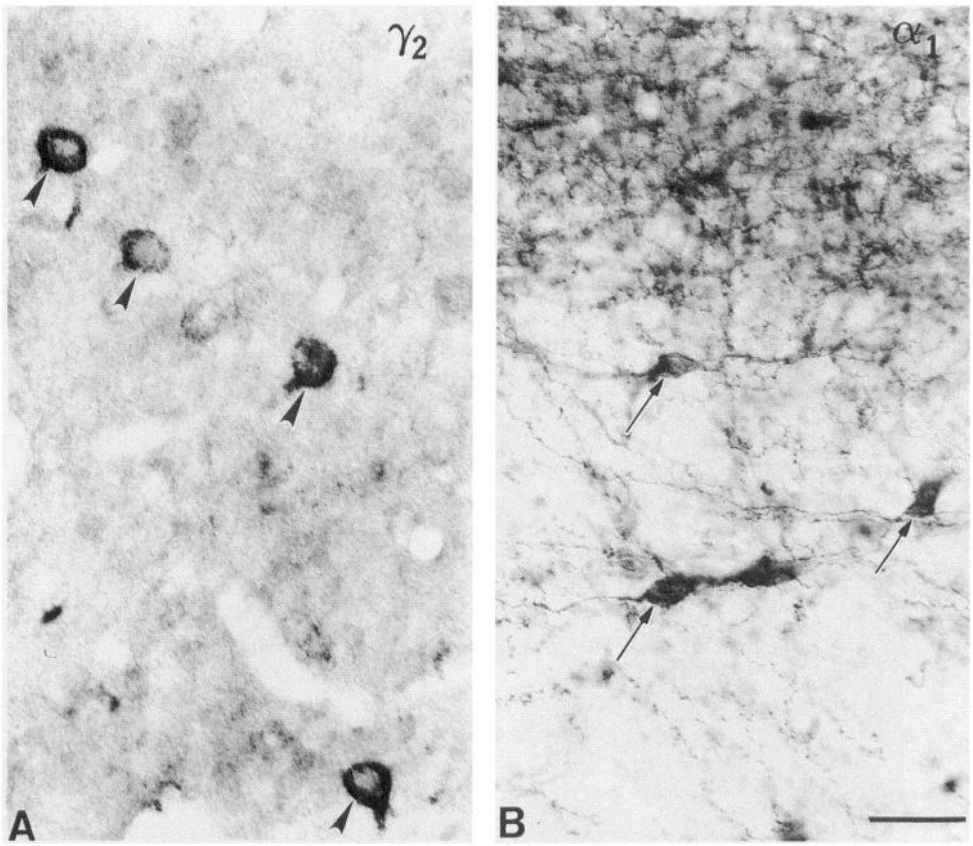

Figure 10. High-magnification photomicrographs of $GABA_A$ receptor immunostaining in human visual cortex. *A*, Immunostaining for $\gamma 2$ in layer IVB of human visual cortex. Several somata (*arrowheads*) display intense cell-surface immunostaining. *B*, Immunostaining for $\alpha 1$ at the border between layer VI and the white matter. Neuronal somata (*arrows*) and their processes in this region display intense cytoplasmic immunostaining. Scale bar, 75 μm.

tribution in the human visual cortex is similar to that in monkeys, and that all three subunits respond identically and, as closely as we can determine, simultaneously to the loss of visual input from one eye. These observations suggest that the combinations $\alpha 1\beta 2\gamma 2$ and/or $\alpha 1\beta 3\gamma 2$ are commonly assembled by primate visual cortical neurons and that they are regulated by the same neuronal mechanisms. Recent studies of rat cerebral cortex demonstrate that the $\alpha 1$, $\beta 2/3$, and $\gamma 2$ subunits frequently coexist in purified receptor complex (Benke et al., 1991b; Khan et al., 1992) and are colocalized in single neurons (Fritschy et al., 1992). The presence of $\alpha 1$, $\beta 2/3$, and $\gamma 2$ subunits in the narrow confines of layer IVA and layer IVC lattices in monkeys and humans and the simultaneous immunofluorescent detection of $\alpha 1$ and $\beta 2/3$ in the same elements of monkey cortex indicate these subunits coexist in neurons of primate area 17. *In vitro* expression studies indicate that combination of $\alpha 1$, $\beta 2$, or $\beta 3$ and $\gamma 2$ confers the full range of physiological activity to $GABA_A$ receptors and that the receptors display typical benzodiazepine I pharmacology (Olson and Tobin, 1990; Burt and Kamatchi, 1991). It is assumed that where $\alpha 1$, $\beta 2/3$, and $\gamma 2$ subunits are unevenly distributed or where other variants of α, β, or γ or another subunit, δ, are expressed by visual cortical neurons, the physiological and pharmacological properties of the $GABA_A$ receptors will vary.

Subunit distribution in monkey area 17

Previous studies of $GABA_A$ receptor localization in macaque area 17 have identified a markedly uneven laminar distribution, with the greatest density of sites that bind muscimol or flunitrazepam in layers II–III and IVC and moderate densities in layer VI (Shaw and Cynader, 1986; Rakic et al., 1988; Hendry et al., 1990). Comparison of immunocytochemical staining patterns in the present study indicates that the $\alpha 1$, $\beta 2/3$, and $\gamma 2$ subunit variants adopt a very similar distribution, including the presence of intense immunoreactivity in each of the layers that display high densities of ligand binding and, in addition, in layer IVA. These patterns of receptor localization follow the pattern of GABA terminal localization (Hendrickson et al., 1981; Fitzpatrick et al., 1987; Hendry et al., 1987), indicating that the major inhibitory neurotransmitter in monkey visual cortex and its principal receptor complex are closely matched.

Except for the somata and processes of neurons in the white matter, cell bodies and dendrites were not immunostained for $\alpha 1$ or $\beta 2/3$ in monkey area 17. Instead, the immunostaining consisted principally of tiny punctate profiles scattered throughout the neuropil and of thin profiles that outlined most circular or oblong unstained regions. These unstained regions were identified as neuronal somata, by their immunoreactivity for the neuron-specific marker MAPs. Much of the $\gamma 2$ immunostaining was similar in its distribution within the neuropil. Such a pattern, with its emphasis on no particular cell type or neuronal element, was one that was expected, given the very large number of synapses formed by GABA terminals and their diverse targets in monkey area 17 (Hendrickson et al., 1981; Fitzpatrick et al., 1987). Thus, even though GABA terminals in monkey area 17 synapse most often upon pyramidal cells, that innervation is not targeted specifically at the somata and primary dendrites of pyramidal cells but is densest on smaller, more peripheral dendrites (Beaulieu et al., 1992). Our finding that receptor subunit immunostaining was densest in regions that contained clusters of thin, presumably peripheral dendrites, is consistent with the quantitative results.

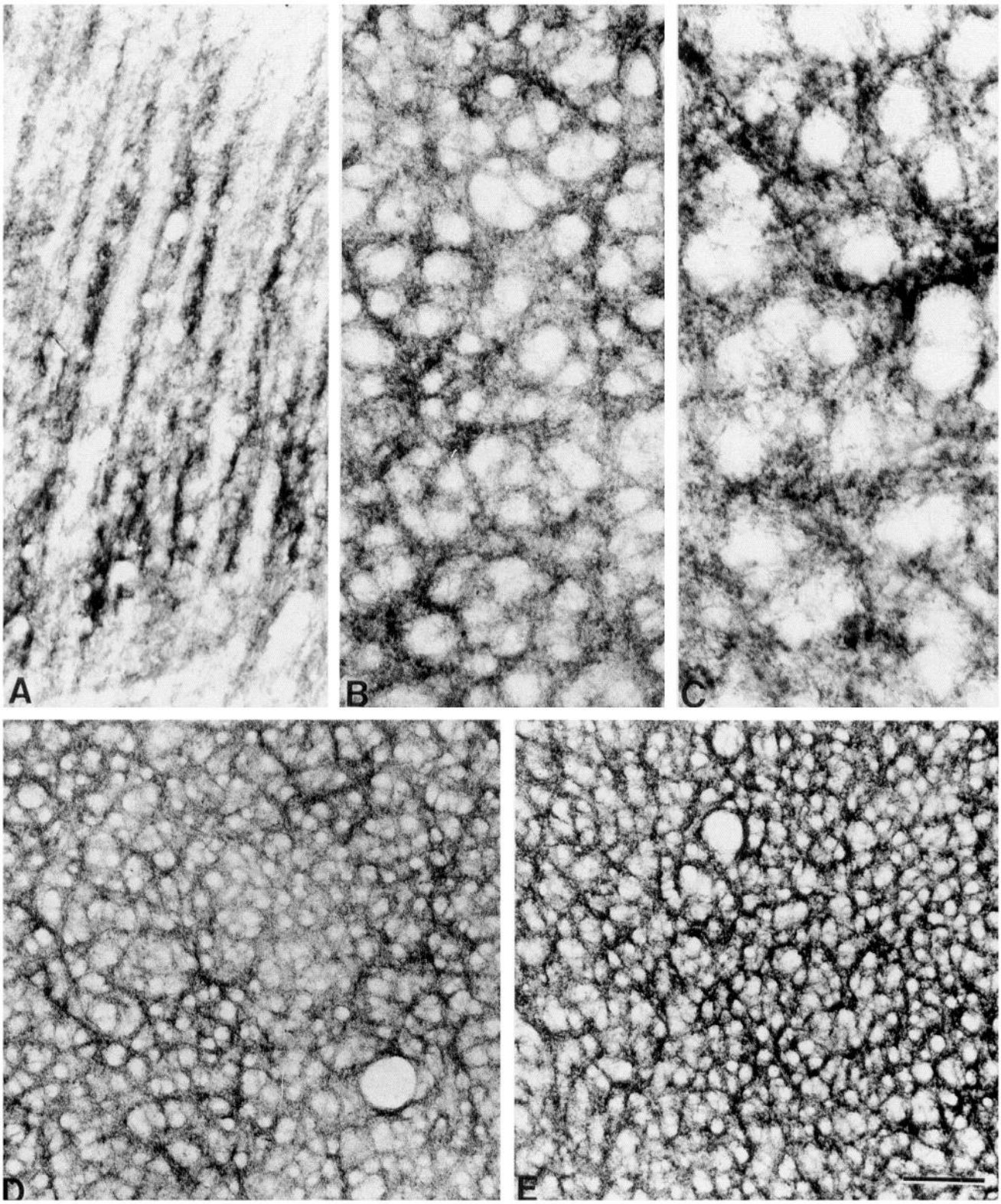

Figure 11. Pattern of β2/3 immunostaining in layer IVCβ of human visual cortex. *A*, Photomicrograph of immunostained layer IVCβ in a section cut along radial lines. Intense immunostaining is present in elongated stripes that are wider and more closely spaced in the deep half of layer IVCβ than in the superficial half. *B* and *C*, High-magnification photomicrographs of β2/3 immunostaining in tangential sections through layer IVCβ. Intense immunostaining is present in clusters that surround circular unstained regions, interpreted as the somata of unstained neurons (*B*). In the clusters are immunostained punctate profiles that vary in size and staining intensity. *D* and *E*, Low-magnification photomicrographs of the patterns formed by β2/3 immunostaining in the superficial (*D*) and deep (*E*) parts of layer IVCβ. In the more superficial part of this layer (*D*), the immunostaining appears as a lattice or honeycomb, in which intensely immunoreactive walls surround lightly stained lacunae. In the deeper part of layer IVC, a finer grained lattice of more intense immunostaining is present. Scale bar: 75 μm for *A*, 35 μm for *B*, 25 μm for *C*, 100 μm for *D* and *E*.

Immunoreactivity for the γ2 subunit in monkey area 17 was located not only in the neuropil but also intensely around the somata of a subpopulation of GABA neurons. The cellular location of the immunoreactivity and its appearance around the individual somata closely resemble the patterns observed for immunostaining with antibodies against certain uncharacterized antigens (Hendry et al., 1984; Hockfield et al., 1984; DeYoe et al., 1990) and the binding of certain lectins (Mulligan et al., 1989) in the monkey visual cortex. A similar pattern of pericellular immunostaining can result from the inadvertent localization of an epitope present in the carrier protein keyhole limpet hemocyanin used in the original immunogen (Mulligan et al., 1992). However, cell surface immunoreactivity in the present study was produced with an anti-γ2 antiserum purified by affinity chromatography. In addition, the anti-γ2 antiserum recognizes a single protein band from monkey brain with an apparent molecular weight identical to that of γ2 in other species. These data indicate the surface immunostaining produced with the anti-g2 antiserum arises from recognition of an epitope on the γ2 subunit, itself. Similarly intense surface immunostaining for other $GABA_A$ receptor subunits has been noted previously for neurons of cat visual cortex (Somogyi, 1989).

Previous studies have noted the frequent extrasynaptic location of $GABA_A$ receptor subunits in mammalian cerebral and cerebellar cortex (de Blas et al., 1988; Somogyi, 1989; Somogyi et al., 1989). Receptor immunoreactivity has been localized to axons (de Blas et al., 1988) and to nonsynaptic regions of somata and dendrites (Somogyi, 1989; Somogyi et al., 1989). The γ2 surface immunoreactivity in monkey and human visual cortex also appears to be extrasynaptic, with densest immunostaining surrounding regions that resemble zones of axosomatic contact.

Comparison of $GABA_A$ receptor subunits in human and monkey visual cortex

Studies that have addressed the organization and neurochemical characteristics of the human primary visual cortex have stressed its similarity to monkey primary visual cortex. As in monkeys, area 17 in humans contains patches or puffs of intense CO activity in layers II–III, IVB, and VI and displays a regular pattern of ocular dominance columns in layer IVC (Horton and Hedley-White, 1984). Patterns of immunocytochemically detected proteins are also similar in the two species (Campbell and Morrison, 1989; Gaspar et al., 1989; Blümcke et al., 1990; Mesulam et al., 1992). The findings of the present study indicate that the distribution of $GABA_A$ receptors is similar in area 17 of monkeys and humans, with a closely matching laminar distribution of all three subunits examined. That similarity extends to the presence of compartments in layer IVC, composed of alternating intensely stained and poorly stained stripes. Through

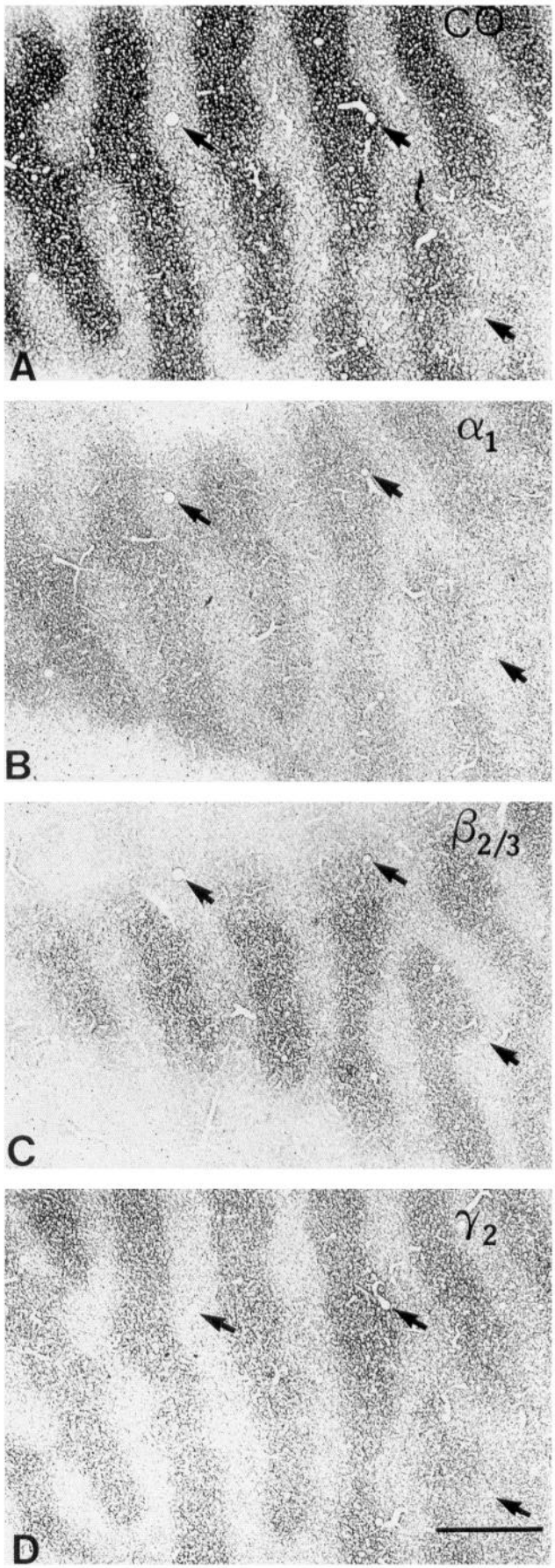

→

Figure 12. Reduction in $GABA_A$ receptor subunit immunoreactivity in layer IVC of an adult monkey monocularly deprived for 5 d by a single intravitreal injection of TTX. *A*, Photomicrograph of a section stained histochemically for CO. Alternating darkly and lightly stained stripes correspond to normal- and deprived-eye columns, respectively. *B–D*, Photomicrographs of sections adjacent that in *A*, showing dark and light stripes immunostained for α1 (*B*), β2/3 (*C*), and γ2 (*D*). Comparison of the same blood vessel profiles (*arrows*) shows that the intensely immunostained stripes are aligned with one another and with the stripes intensely stained for CO, while the lightly immunostained and lightly CO-stained stripes are aligned with another. Scale bar, 1.2 mm.

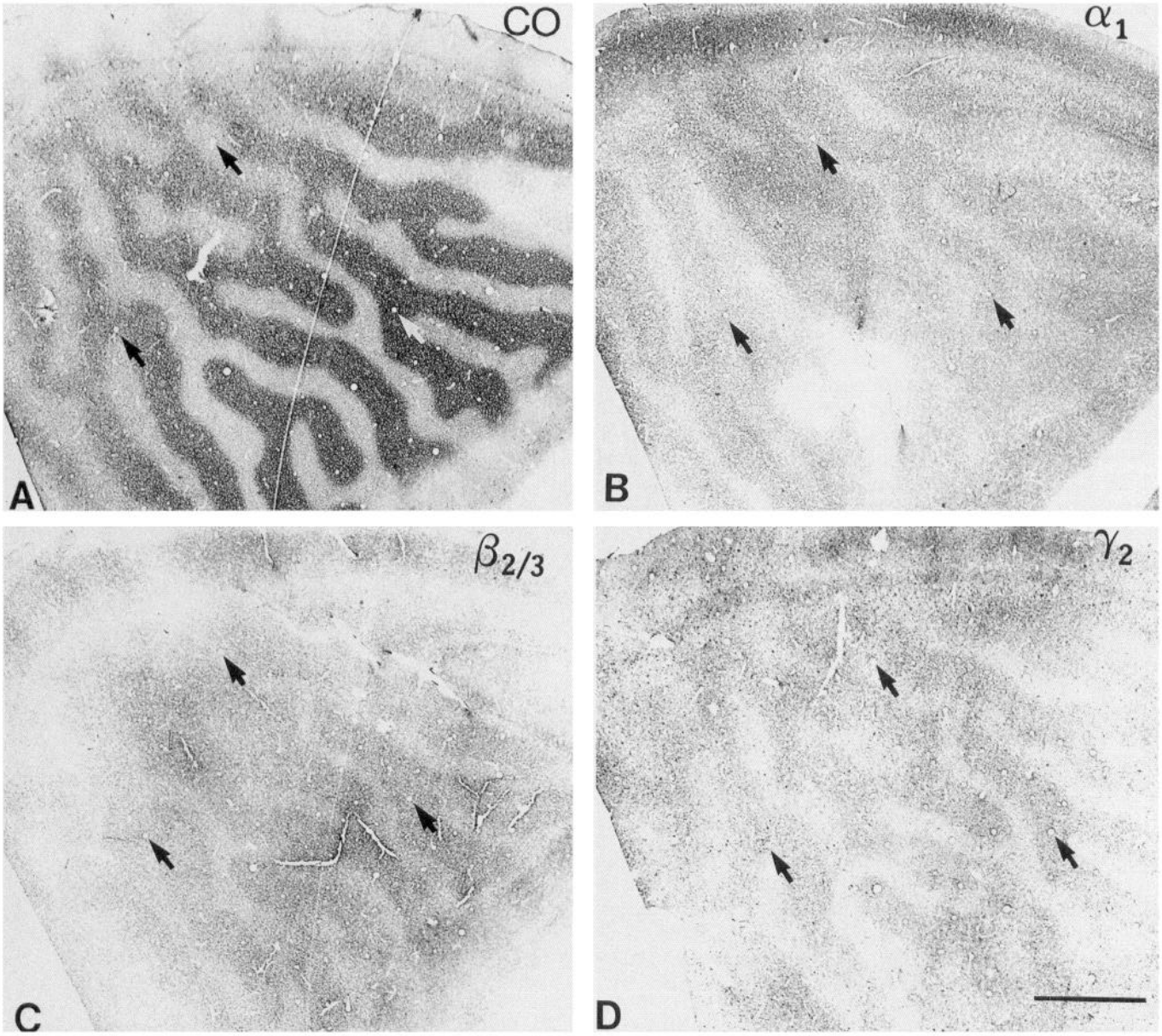

Figure 13. Reduction in $GABA_A$ receptor immunoreactivity following relatively long-term (30 d) monocular deprivation. *A*, Photomicrograph of a tangential section through layer IVC, stained histochemically for CO. Alternating darkly and lightly stained stripes correspond to normal- and deprived-eye columns, respectively. *B–D*, Photomicrographs of adjacent sections immunostained for $\alpha 1$ (*B*), $\beta 2/3$ (*C*), and $\gamma 2$ (*D*). Alternating intensely and lightly immunostained stripes are evident in all sections. Comparison of the positions of the same blood vessel profiles (*arrows*) shows that the dark CO stripes are aligned with the intensely immunostained strips while the light CO stripes are aligned with the lightly immunostained stripes. Scale bar, 1.9 mm.

the full thickness of layer IVC in monkey visual cortex the stripes appear in tangential sections as a fine lattice (Hendry et al., 1990). In human area 17, the receptor immunostaining forms different types of lattices in lower IVCβ and upper IVCβ, with the more superficial and loosely organized lattice closely resembling the pattern seen in layer IVA of monkeys. Such a pattern is directly related to geniculocortical (Hubel and Wiesel, 1972; Hendrickson et al., 1978) and intrinsic GABAergic terminations (Fitzpatrick et al., 1987) in monkey visual cortex and might be similarly related in human area 17. The most compelling findings were not the differences but the similarities in area 17 of humans and monkeys, and how closely the two resemble the first somatic sensory area and precentral motor area of monkeys (Huntley et al., 1990), since all three display the common pattern of radial stripes of $GABA_A$ receptors. Such a pattern appears related to the segregation of intrinsic and thalamocortical inputs, not only in layer IVA of monkey area 17, but also in layer IVC, where immunostained thalamocortical and GABAergic terminals occupy clusters (DeFelipe and Jones, 1991), similar to the ones seen immunostained for the $GABA_A$ receptor subunits (Hendry et al., 1990). These data suggest that compartments made up of clusters or lattices may be a common feature of principal thalamocortical-recipient layers in sensory areas of both monkey and human cerebral cortex.

Layer IVA of the human visual cortex is unlike that of the monkey in exhibiting no evidence of intense histochemical

staining for CO (Horton and Hedley-White, 1984; Wong-Riley et al., 1993), a finding that suggests this layer might vary fundamentally between the two species, perhaps as a target of geniculocortical axons in monkeys and not in humans. However, layer IVA has the same cytoarchitecture in the two species, with a distinct group of small, closely spaced somata (Brodmann, 1909). The present study also suggests that at least for the distribution of $GABA_A$ receptors, layer IVA in monkeys and humans is neurochemically similar since relatively intense immunoreactivity for the $\alpha 1$, $\beta 2/3$, and $\gamma 2$ subunits of the $GABA_A$ receptor is present in both.

Patches of intense receptor immunostaining were detected in layers II–III of monkey visual cortex, which correspond to the regions of the CO puffs (Horton and Hubel, 1981; Wong-Riley and Carroll, 1984; Hendrickson, 1985). These are innervated by a distinct group of geniculocortical neurons (Fitzpatrick et al., 1983; Horton, 1984; Livingstone and Hubel, 1984) and display heightened immunostaining for GAD (Hendrickson et al., 1981) due to the presence of large GABAergic terminals (Fitzpatrick et al., 1987). The localization of intense immunoreactivity for the $\alpha 1$, $\beta 2/3$, and $\gamma 2$ subunits to the puffs in monkey area 17 suggests that relative densities of GABA terminals and functional $GABA_A$ receptors are matched in these regions. The failure to detect a patchy distribution of receptor immunoreactivity in human area 17 may be indicative of a basic difference in $GABA_A$ receptor distribution in monkeys and humans, or it may be due to the methods we found necessary in studying human cortex, including relatively long fixation times and relatively thick sections.

Regulation of subunit immunoreactivity

Loss of vision in one eye leads to rapid reductions in immunoreactivity for GABA and GAD in neurons within deprived-eye columns of the adult monkey visual cortex (Hendry and Jones, 1986, 1988). The reduction in both immunostained somata and terminals appears to reflect an activity-dependent regulation of GAD within neurons deprived of normal visual input. A parallel reduction in immunoreactivity for the $\beta 2/3$ subunits and in the binding of radiolabeled muscimol and flunitrazepam indicated previously that $GABA_A$ receptors were also downregulated in response to monocular deprivation (Hendry et al., 1990). However, the complex biochemical composition of the $GABA_A$ receptor potentially could allow for changes in other subunits that might compensate for a reduction in $\beta 2/3$ subunits. For example, reductions in the number of β-subunits and their constituent GABA binding sites could be matched by compensatory changes in α- or γ-subunits, which normally regulate the binding and efficacy of benzodiazepines (Levitan et al., 1988a,b; Prichett et al., 1989; Malherbe et al., 1990a,b). The present findings demonstrate that for all three variants examined, $\alpha 1$, $\beta 2/3$, and $\gamma 2$, monocular deprivation in adulthood leads to marked reductions in immunoreactive levels within deprived-eye columns. These changes in immunoreactivity appear to depend on reduced gene expression for each of the subunits as determined by *in situ* hybridization histochemistry (Huntsman et al., 1992). The findings provide further evidence that GABA-mediated inhibition is likely to be reduced within the visual cortical regions dominated by a deprived eye.

Fully functional $GABA_A$ receptors, which display cooperativity of GABA binding and benzodiazepine-mediated increases in the affinity of the receptor complex for GABA, require α-, β-, and γ-subunits (Prichett et al., 1989; Sigel et al., 1990; Moss et al., 1991). Yet each of these subunit classes includes several distinct variants (Sieghart, 1989; Olsen and Tobin, 1990). Therefore, deprivation-induced reduction in immunoreactive levels of one subunit variant (e.g., $\alpha 1$) might be accompanied by increased immunoreactive levels for other variants ($\alpha 2$–6) of the same subunit class. Studies of properties displayed by different subunit combinations in expression systems suggest that a replacement of this type alters the physico-pharmacological properties of the receptor complex. For example, in an $\alpha\beta\gamma$ combination, substitution of $\alpha 2$, -3, or -5 for $\alpha 1$ changes the properties of the combined receptor complex from benzodiazepine type I to benzodiazepine type II (Pritchett et al., 1989a; Seeburg et al., 1990; Lüddens and Wisden, 1991). Such a change might account for the altered binding of flunitrazepam and the GABA agonist muscimol that was found previously in deprived-eye columns of monkey area 17 (Hendry et al., 1990). Further studies devoted to examining all variants of a single receptor subunit class will be necessary to determine if reduced immunoreactivity for $\alpha 1$, $\beta 2/3$, and $\gamma 2$ occurs with changes in the concentration of other variants in these same classes.

Whereas most research over the past two decades has led to the conclusion that the visual cortex of adult monkeys displays little functional plasticity when deprived of normal, binocular vision (Hubel and Wiesel, 1977; Hubel et al., 1977; von Noorden and Crawford, 1978; LeVay et al., 1980), recent studies have found dramatic evidence for functional rearrangement in the visual cortex of adult cats and monkeys following manipulations of both eyes. These studies have shown that laser lesions in corresponding parts of the two retinas or lesions in one eye followed by enucleation of the other eye produce initial silent zones in area 17 followed by expansion into them of the bordering visual field representation (Kaas et al., 1990; Heinen and Skavenski, 1991; Gilbert and Wiesel, 1992). Similar expansions were reported earlier in the LGN of the cat (Eysel et al., 1980, 1981; Eysel, 1982), but the size and speed of the cortical enlargement and the persistence of an LGN silent zone after the cortical rearrangement has taken place (Gilbert and Wiesel, 1992) argue against a thalamic mechanism for the observed plasticity. One obvious conclusion of the present study is that intracortical mechanisms that underlie the functional adaptability of the adult visual cortex may include activity-dependent changes in neurotransmitter and receptor levels that modify the efficacy of existing cortical connections.

References

Alger BE (1985) GABA and glycine: postsynaptic actions. In: Neurotransmitter actions in the vertebrate nervous system (Rogawski MA, Barker JL, eds), pp 33–69. New York: Plenum.

Barnard EA, Darlison MG, Seeburg P (1987) Molecular biology of the $GABA_A$ receptor/channel superfamily. Trends Neurosci 10:502–509.

Beaulieu C, Kisvarday Z, Somogyi P, Cynader M, Cowey A (1992) Quantitative distribution of GABA-immunopositive and -immunonegative neurons and synapses in the monkey striate cortex (area 17). Cereb Cortex 2:295–309.

Benke D, Mertens S, Möhler H (1991a) Ubiquitous presence of $GABA_A$ receptors containing the $\alpha 1$ subunit in rat brain demonstrated by immunoreprecipitation and immunohistochemistry. Mol Neuropharmacol 1:103–110.

Benke D, Mertens S, Trzeciak D, Gillessen D, Möhler H (1991b) $GABA_A$ receptors display association of $\gamma 2$-subunit with $\alpha 1$ and $\beta 2/3$ subunits. J Biol Chem 266:4478–4483.

Blümcke I, Hof PR, Morrison JH, Celio MR (1990) Distribution of parvalbumin immunoreactivity in the visual cortex of Old World monkeys and humans. J Comp Neurol 301:417–432.

Bowery NG, Pratt GD, Knott C (1990) $GABA_B$ receptors: past, present

and future. In: $GABA_B$ receptors in mammalian function (Bowery NG, Bittiger H, Olpe H, eds), pp 3–28. New York: Wiley.
Brodmann K (1909) Vergeleichende Lokalisationslehre der Großhirnrinde in ihren Prinzipien dargesteldt auf Grund des Zellenbaus. Leipzig: Barth.
Burt DR, Kamatchi GL (1991) $GABA_A$ receptor subtypes: from pharmacology to molecular biology. FASEB J 5:2916–2923.
Campbell MJ, Morrison JH (1989) Monoclonal antibody to neurofilament protein (SMI-32) labels a subpopulation of pyramidal neurons in the human and monkey neocortex. J Comp Neurol 282:191–205.
Cutting G, Lu L, O'Hara BF, Kasch LM, Montrose-Rafizadeh C, Donovan DM, Shimada S, Antonarakis SE, Guggino WB, Uhl GR, Kazazian HH Jr (1991) Cloning of the γ-aminobutyric acid (GABA) ρ1 cDNA: a GABA receptor subunit highly expressed highly expressed in the retina. Proc Natl Acad Sci USA 88:2673–2677.
de Blas AL, Vitorica J, Friedrich P (1988) Localization of the $GABA_A$ receptor in the rat brain with a monoclonal antibody to the 57,000 M_r peptide of the $GABA_A$ receptor/benzodiazepine receptor/Cl^- channel complex. J Neurosci 8:602–614.
DeFelipe J, Jones EG (1991) Parvalbumin immunoreactivity reveals layer IV of monkey cerebral cortex as a mosaic of microzones of thalamic afferent terminations. Brain Res 562:39–47.
DeYoe EA, Hockfield S, Garren H, Van Essen DC (1990) Antibody labeling of functional subdivisions in visual cortex: Cat-301 immunoreactivity in striate and extrastriate cortex of the macaque monkey. Vis Neurosci 5:67–81.
Eysel U (1982) Functional reconnections without new axonal growth in a partially denervated visual relay nucleus. Nature 299:442–444.
Eysel UT, Gonzalez-Aguilar F, Mayer U (1980) A functional sign of reorganization in the visual system of adult cats: lateral geniculate neurons with displaced receptive fields after lesions of the nasal retina. Brain Res 181:285–300.
Eysel UT, Gonzalez-Aguilar F, Mayer U (1981) Time-dependent decrease in the extent of visual deafferentation in the lateral geniculate nucleus of adult cats with small retinal lesions. Exp Brain Res 41: 256–263.
Fitzpatrick D, Itoh K, Diamond IT (1983) The laminar organization of the lateral geniculate body and he striate cortex in the squirrel monkey (*Saimiri sciureus*). J Neurosci 3:673–702.
Fitzpatrick D, Lund JS, Schmechel D, Towles AW (1987) Distribution of GABAergic neurons and axon terminals in the macaque striate cortex. J Comp Neurol 264:73–91.
Fritschy JM, Benke D, Mertens S, Oertel WH, Bachi T, Möhler H (1992) Five subtypes of type A gamma-aminobutyric acid receptors identified in neurons by double and triple immunofluorescence staining with subunit-specific antibodies. Proc Natl Acad Sci USA 89: 6726–6730.
Fuchs K, Möhler H, Sieghart W (1988) Various proteins from rat brain, specifically and irreversibly labeled by [^{3}H]flunitrazepam, are distinct α-subunits of the GABA-benzodiazepine receptor complex. Neurosci Lett 90:314–319.
Gaspar P, Berger B, Febvret A, Vigny A, Henry JP (1989) Catecholamine innervation of the human cerebral cortex as revealed by comparative immunohistochemistry of tyrosine hydroxylase and dopamine-beta-hydroxylase. J Comp Neurol 279:249–271.
Gilbert CD, Wiesel TN (1992) Receptive field dynamics in adult primary visual cortex. Nature 356:150–152.
Heinen SJ, Skavenski AA (1991) Recovery of visual responses in foveal V1 neurons following bilateral foveal lesions in adult monkey. Exp Brain Res 83:670–674.
Hendrickson AE (1985) Dots, stripes and columns in monkey visual cortex. Trends Neurosci 8:406–410.
Hendrickson AE, Wilson JR, Ogren MP (1978) The neuroanatomical organization of pathways between dorsal lateral geniculate nucleus and visual cortex in Old and New World primates. J Comp Neurol 182:123–136.
Hendrickson AE, Hunt SP, Wu J-Y (1981) Immunocytochemical localization of glutamic acid decarboxylase in monkey striate cortex. Nature 292:605–607.
Hendry SHC, Jones EG (1986) Reduction in number of GABA immunostained neurons in deprived-eye dominance columns of monkey area 17. Nature 320:750–753.
Hendry SHC, Jones EG (1988) Activity-dependent regulation of GABA expression in the visual cortex of adult monkeys. Neuron 1:701–712.
Hendry SHC, Hockfield S, Jones EG, McKay R (1984) Monoclonal antibody that identifies subsets of neurons in the central visual system of monkey and cat. Nature 307:267–269.
Hendry SHC, Schwark HD, Jones EG, Yan J (1987) Numbers and proportions of GABA immunoreactive neurons in different areas of monkey cerebral cortex. J Neurosci 7:1503–1520.
Hendry SHC, Jones EG, Emson PC, Lawson DEM, Heizmann CW, Streit P (1989) Two classes of cortical GABA neurons defined by differential calcium binding protein immunoreactivities. Exp Brain Res 76:467–472.
Hendry SHC, Fuchs J, de Blas AL, Jones EG (1990) Distribution and plasticity of immunocytochemically localized $GABA_A$ receptors in adult monkey visual cortex. J Neurosci 10:2438–2450.
Hockfield S, McKay RD, Hendry SHC, Jones EG (1984) A surface antigen that identifies ocular dominance columns in the visual cortex and laminar features of the lateral geniculate nucleus. Cold Spring Harbor Symp Quant Biol 35:877–889.
Horton JC (1984) Cytochrome oxidase patches: a new cytoarchitectonic feature of monkey visual cortex. Philos Trans R Soc Lond [Biol] 304:199–253.
Horton JC, Hedley-White ET (1984) Mapping of cytochrome oxidase patches and ocular dominance columns in human visual cortex. Philos Trans R Soc Lond [Biol] 304:255–272.
Horton JC, Hubel DH (1981) Regular patchy distribution of cytochrome oxidase staining in primary visual cortex of macaque monkey. Nature 292:762–764.
Hubel DH, Wiesel TN (1972) Laminar and columnar distribution of geniculo-cortical fibers in the macaque monkey. J Comp Neurol 146: 421–450.
Hubel DH, Wiesel TN (1977) Functional architecture of macaque monkey visual cortex. Proc R Soc Lond [Biol] 198:1–59.
Hubel DH, Wiesel TN, LeVay S (1977) Plasticity of ocular dominance columns in monkey striate cortex. Philos Trans R Soc Lond [Biol] 278:377–409.
Huntley GW, deBlas AL, Jones EG (1990) $GABA_A$ receptor immunoreactivity in adult and developing monkey sensory-motor cortex. Exp Brain Res 82:519–535.
Huntsman MM, Jones EG, Möhler H, Hendry SHC (1991) Distribution of immunocytochemically localized $GABA_A$ receptor subunits in monkey and human visual cortex. Soc Neurosci Abstr 17:115.
Huntsman MM, Isackson PJ, Jones EG (1992) Differential regulation of $GABA_A$ receptor subunit mRNAs in adult monkey visual cortex by monocular deprivation. Soc Neurosci Abstr 18:299.
Kaas JH, Krubitzer LA, Chino YM, Langston AL, Polley EH, Blair N (1990) Reorganization of retinotopic cortical maps in adult mammals after lesion of the retina. Nature 248:229–231.
Khan ZV, Fernando LP, Escriba P, Busquets X, Mallet J, Miralles C, Filla M, de Blas AL (1992) Antibodies to the human γ2 subunit of the $GABA_A$/benzodiazepine receptor. J Neurochem 60:961–971.
Khrestchatisky M, MacLennan A, Chiang MY, Xu W, Jackson M, Brecha N, Strenini C, Olsen R, Tobin A (1989) A novel a subunit in rat brain $GABA_A$ receptors. Neuron 3:745–753.
Klein WL, Sullivan J, Skorupa A, Aguilar JS (1989) Plasticity of neuronal receptors. FASEB J 3:2132–2140.
Krnjević K (1984) Neurotransmitters in cerebral cortex: a general account In: Cerebral cortex, Vol 2, Functional properties of cortical cells (Jones EG, Peters A, eds), pp 39–61. New York: Plenum.
LeVay S, Wiesel TN, Hubel DH (1980) The development of ocular dominance columns in normal and visually deprived monkeys. J Comp Neurol 191:1–51.
Levitan E, Blair L, Dionne V, Barnard E (1988a) Biophysical and pharmacological properties of cloned $GABA_A$ receptor subunits expressed in *Xenopus* oocytes. Neuron 1:773–781.
Levitan E, Schofield P, Burt D, Rhee L, Wisden W, Köhler M, Fujita N, Rodriguez H, Stephenson A, Darlison M, Barnard E, Seeburg P (1988b) Structural and functional basis for $GABA_A$ receptor heterogeneity. Nature 335:76–79.
Livingstone MS, Hubel DH (1984) Anatomy and physiology of a color system in the primate visual cortex. J Neurosci 4:309–356.
Lømo T, Rosenthal J (1972) Control of ACh sensitivity by muscle activity in the rat. J Physiol (Lond) 221:493–513.
Lüddens H, Wisden W (1991) Function and pharmacology of multiple $GABA_A$ receptor subunits. Trends Pharmacol Sci 12:49–51.
Malherbe P, Sigel E, Baur R, Persohn E, Richards JG, Möhler H (1990a) Functional characteristics and sites of gene expression of the α1β1γ1 isoform of the rat $GABA_A$ receptor. J Neurosci 10:2330–2337.
Malherbe P, Sigel E, Baur R, Richards JG, Möhler H (1990b) Func-

tional expression and sites of transcription of a novel α-subunit of the GABA receptor in rat brain. FEBS Lett 260:261–265.

Mesulam M-M, Hersh LB, Mash, DC, Geula C (1992) Differential cholinergic innervation within functional subdivisions of the human cerebral cortex: a choline acetyltransferase study. J Comp Neurol 318: 316–328.

Miledi R (1960) The acetylcholine sensitivity of frog muscle fibres after complete or partial denervation. J Physiol (Lond) 151:1–23.

Moss S, Ravindran A, Mei L, Wang JB, Kofiji P, Huganir R, Burt D (1991) Characterization of recombinant $GABA_A$ receptors produced in transfected cells from murine $\alpha 1$, $\beta 1$, and $\gamma 2$ subunit cDNAs. Neurosci Lett 123:265–268.

Mulligan KA, Van Brederode JFM, Hendrickson AE (1989) The lectin *Vicia villosa* labels a distinct subset of GABAergic cells in macaque visual cortex. Vis Neurosci 2:63–72.

Mulligan KA, Van Brederode JFM, Mehra R, Hendrickson AE (1992) VVA-labelled cells in monkey visual cortex are double-labelled by a polyclonal antibody to a cell surface epitope. J Neurocytol 21:244–259.

Olsen RW, Tobin AJ (1990) Molecular biology of $GABA_A$ receptors. FASEB J 4:1469–1480.

Olsen RW, Venter JC (1986) Benzodiazepine/GABA receptors and chloride channels: structural and functional properties. In: Receptor biochemistry and methodology (Olsen RW, Venter JC, eds), pp 4–30. New York: Liss.

Pritchett D, Luddens H, Seeburg P (1989a) Type I and type II $GABA_A$ benzodiazepine receptors produced in transfected cells. Science 246: 1389–1392.

Prichett D, Sontheimer H, Shivers B, Ymer S, Kettenmann H, Schofield P, Seeburg P (1989b) Importance of a novel $GABA_A$ receptor subunit for benzodiazepine pharmacology. Nature 338:582–585.

Rakic P, Goldman-Rakic PS, Gallagher D (1988) Quantitative autoradiography of major neurotransmitter receptors in the monkey striate and extrastriate cortex. J Neurosci 8:3670–3690.

Schofield PR (1989) The $GABA_A$ receptor: molecular biology reveals a complex picture. Trends Pharmacol Sci 10:476–478.

Seeburg PH, Wisden W, Verdoon TA, Pritchett DB, Werner P, Herb A, Luddens H, Sprengel R, Sakmann B (1990) The $GABA_A$ receptor family: molecular and functional diversity. Cold Spring Harbor Symp Quant Biol 55:29–40.

Shaw C, Cynader M (1986) Laminar distribution of receptors in monkey (*Macaca fascicularis*) geniculostriate system. J Comp Neurol 248: 301–312.

Shivers B, Killisch I, Sprengel R, Sontheimer H, Köhler M, Schofield P, Seeberg P (1989) Two novel $GABA_A$ receptor subunits exist in distinct neuronal subpopulations. Neuron 3:327–337.

Sieghart W (1989) Multiplicity of $GABA_A$-benzodiazepine receptors. Trends Pharmacol Sci 10:407–411.

Sigel E, Baur R, Trube G, Möhler H, Malherbe P (1990) The effect of subunit composition of rat brain $GABA_A$ receptors on channel function. Neuron 5:703–711.

Somogyi P (1989) Synaptic organization of GABAergic neurons and $GABA_A$ receptors in the lateral geniculate nucleus and visual cortex. In: Neural mechanisms of visual perception (Lam DM-K, Gilbert CD, eds), pp 35–62. Houston: Portfolio.

Somogyi P, Takagi H, Richards JG, Möhler H (1989) Subcellular localization of benzodiazepine/$GABA_A$ receptors in the cerebellum of rat, cat and monkey using monoclonal antibodies. J Neurosci 9:2197–2209.

Stephenson A (1988) Understanding the $GABA_A$ receptor: a chemically gated ion channel. Biochem J 249:21–32.

Van Brederode JFM, Mulligan KA, Hendrickson AE (1990) Calcium-binding proteins as markers for subpopulations of GABAergic neurons in monkey striate cortex. J Comp Neurol 298:1–22.

Vitorica J, Park D, Chin G, de Blas AL (1988) Monoclonal antibodies and conventional antisera to the $GABA_A$ receptor/benzodiazapine receptor/Cl^- channel complex. J Neurosci 2:615–622.

von Noorden GK, Crawford MLJ (1978) Morphological and physiological changes in the monkey visual system after short-term lid suture. Invest Ophthalmol Vis Sci 17:762–768.

Wisden W, Laurie DJ, Monyer H, Seeburg PH (1992) The distribution of 13 $GABA_A$ receptor subunit mRNAs in the rat brain. I. Telencephalon, diencephalon and mesencephalon. J Neurosci 12:1040–1062.

Wong-Riley M, Carroll EW (1984) Effect of impulse blockage on cytochrome oxidase activity in monkey visual system. Nature 307:262–264.

Wong-Riley MTT, Hevner RF, Cutlan R, Earnest M, Egan R, Frost J, Nguyen T (1993) Cytochrome oxidase in the human visual cortex: distribution in the developing and the adult brain. Vis Neurosci 10: 41–58.

Zezula J, Cortes R, Probst A, Palacios JM (1988) Benzodiazepine receptor sites in the human brain: autoradiographic mapping. Neuroscience 25:771–795.